Part II

Evaluation of Relay Dynamic Response by Utilizing Co-simulation Platform (PSS/E- CAPE)

and

Loss of Excitation Detection Algorithm to Prevent LOE Relay Mis-operation during Power Swing

Iman Kiaei
Saeed Lotfifard
Anjan Bose

Washington State University

For information about this project, contact

Saeed Lotfifard, Project Leader
School of Electrical Engineering and Computer Science
Washington State University
Pullman, WA 99164-2752
Phone: 509-335-0903
Email: s.lotfifard@wsu.edu

Power Systems Engineering Research Center

The Power Systems Engineering Research Center (PSERC) is a multi-university Center conducting research on challenges facing the electric power industry and educating the next generation of power engineers. More information about PSERC can be found at the Center's website: http://www.pserc.org.

For additional information, contact:

Power Systems Engineering Research Center
Arizona State University
527 Engineering Research Center
Tempe, Arizona 85287-5706
Phone: 480-965-1643
Fax: 480-727-2052

Notice Concerning Copyright Material

Table of Contents

List of Figures

List of Tables

1. Introduction

1.1 Background

The investigations on the major disturbances and outages during the last decades have shown that significant blackouts had triggered due to the variety of factors such as human mistakes, extreme weather events, imbalance of generation and demand, congestion and overloading on the transmission paths, inaccurate calibration of the protective devices and etc.[1]. The North American Electric Reliability Corporation (NERC) concluded that the August 14, 2003 blackout was triggered by a simple natural cause and exacerbated by mis-operations of protective relays that ultimately led to a cascading failure phenomenon [1]. Inaccurate relay settings and coordination may lead to widespread outages with millions of people losing power. The protective devices may not operate correctly based on the steady state settings during the transient conditions. Protective relay mis-operation can be in the following forms [2]:

1. The protective relay fails to operate within a specified time interval when a fault occurs inside the protection zone (i.e. dependability issue)
2. The protective relay operates in the case of faults that are not in the protection zone (i.e. selectivity issue)
3. The protective relay operates when there is no fault in the system (i.e. security issue).

After large disturbances in power systems, the system tries to adjust and settle to the new stable condition. Therefore the system frequency starts to oscillate in different part of the system which results in the amplitude and phase angle of voltages and currents swing. In consequence the impedance measurements based on the varying voltages and currents will also oscillate. During the power swing, the impedance-based protection relays may mis-operate in the non-faulty condition. In swing condition, the impedance trajectory seen by a relay may traverse inside the mho characteristic of the distance element in impedance relays or loss of excitation (LOE) relays and leads to mis-trip [3]. This mis-operation is expressed as one of the fundamental factor of initiating and widening the blackouts [4]. According to literature more than %70 of immense power outages triggered by relay mis-operations which most of these unwanted operations are caused by the distance element in various types of relays such as distance/impedance relay and LOE relay [**Error! Bookmark not defined.**, 5- 6]. Thus, different strategies have been proposed to prevent the impedance element mis-operations which will be explained in the following section.

Furthermore, the catastrophic outages demonstrate the importance of testing relays during transients conditions [7]. Protective relays performance indices such as dependability, security, selectivity, and operating time can be verified more accurately during transients [8].

An overview of the methodology for the transient relay testing is described in this part. The dynamic performance of LOE and impedance relays during power swings is investigated. Response of protective relays is demonstrated using CAPE-Transient Stability (CAPE-TS) module that links CAPE software with PSS/E software. In addition, this paper provides a more realistic dynamic simulation of the relay performance characteristics in the large Western Electricity Coordinating Council (WECC) system during the critical outages. The results demonstrate a

system with a large disturbance and a subsequent protective and remedial action schemes (RAS) may not be successful in preventing cascading outages because of relay mis-operation, and the system eventually breaks up into several parts as a results of unintentional islanding. Also, an adaptive technique is proposed which can distinguish LOE and swing conditions and prevent mis-operation.

1.2 Distance/Impedance Relay Mis-operation

Transmission lines are equipped with distance relays. During the swing cycle, the load impedance, which is outside the relay's protection zones under the steady state, may traverse into the distance relay mho characteristic and causes relay mis-operations.

According to Figure 1.1, the apparent impedance seen by distance element of the relay at point A is as follows [3]:

$$Z_A = \frac{(Z_S + Z_L + Z_R)}{2} \times \left(\frac{k\left[(k - \cos\delta) - j\sin\delta\right]}{(k - \cos\delta)^2 + (\sin\delta)^2} \right) - Z_S \qquad (1.1)$$

Where k is the ratio of the source voltage magnitudes $|E_S|/|E_R|$ and it is assumed E_S (sending source) leads E_R (receiving source) by δ phase.

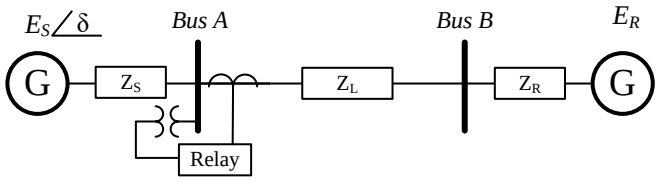

Figure 1.1 Thevenin equivalent circuit of power system

In the power swing cycle, the phase-angle difference of two sources (δ) varies, thus the measured impedance traverses on the R-X plane with respect to the k ratio and where the system electrical center is located. In the equivalent two area power system, when two generators fall out of synchronism (δ =180°), a voltage zero point is created on the tie line between areas which is known as the electrical center [9]. Location of electrical center is affected by the fault location, fault type, network configuration and operating point of the system. The protective relays adjacent to the electrical center are sensitive to the power swings, so if the electrical center of the swing is along the protected line, the apparent impedance trajectory may pass through the protective relay's characteristic.

When E_S is smaller than E_R the trajectory is a circle below the electrical center. When the frequency f_S is larger that f_R the direction of the swing is from right to left, whereas, it will move from left to right if f_S is smaller than f_R. Figure 1.2 illustrates the distance relay mho characteristic and swing impedance loci.

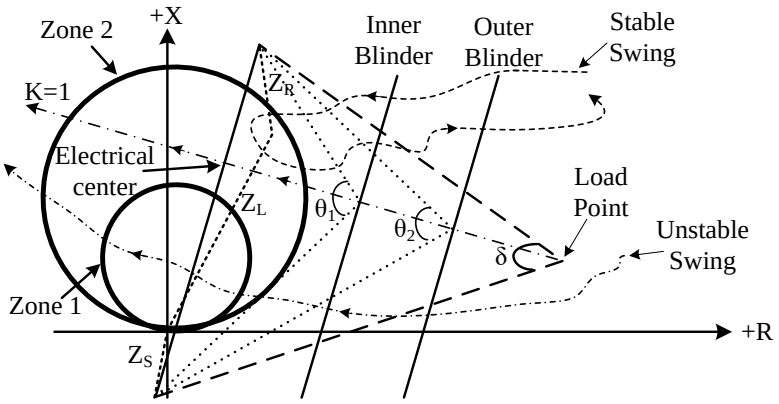

Figure 1.2 Distance relay characteristic and Impedance locus during stable & unstable swing

As shown in Figure 1.2 the distance zones can see some of the power swings (stable or unstable) and can potentially operate and trip the circuit breaker. Some operations may be desired but many will be undesired tripping particularly when the swings are stable. Thus, power swing blocking (PSB) function is utilized in distance relays to prevent unintentional operations during power swings. If the apparent impedance remains between inner and outer blinder elements for a predefined time delay, the PSB recognizes faults from power swing and blocks distance relay elements from operating.

Different methods have been proposed to detect the power swing conditions and prevent the relay mis-operations. These methods include the approaches that are based on rate of change of impedance, rate of change of resistance *dR/dt*, rate of change of swing center voltage (SCV), and rate of change of current [5], [10]. A widely used algorithm operates based on the impedance displacement speed in the R-X plane. The rate of change of impedance seen by the relay depends on the sources, transmission line impedances and the slip frequency ($\omega=d\delta/dt$) which the system is oscillating and expressed as follows [11]:

$$\left|\frac{dZ_A}{dt}\right| = \frac{\left|Z_S + Z_L + Z_R\right|}{(2\sin\frac{\delta}{2})^2} \times \left|\omega\right| \tag{1.2}$$

The conventional method is based on measuring the rate of change of apparent impedance between two right and left impedance elements (blinders). If time interval for crossing between these two predefined blinders exceeds a predefined time period, the relay blocks the distance element during the swing cycle (PSB function) [12]. The inner blinder is determined such that it does not encroach into the most over- reaching mho element and the outer blinder is set to not encroach to the load region with some safety margin [13]. The PSB time delay is determined from the inner and outer blinders setting and the power swing slip rate as follows:

$$PSBD\ (\text{cycle}) = \frac{(\theta_1 - \theta_2) \times F_{nom}}{360^\circ\ f_{stable}} \tag{1.3}$$

Where θ_1, θ_2, F_{nom} and f_{stable} are the machine angles at the outer and inner blinder reaches (degree), system nominal frequency (Hz) and power swing rate (Hz) (which is assumed to be 1.2 Hz), respectively. The blinder schemes are shown in Figure 1.2. Since the inner and outer blinder elements placements depend on the line impedance and equivalent source impedance magnitudes, finding the appropriate setting is challenging [11].

This conventional protection scheme with OSB may also mis-operate if it is not calibrated precisely.

1.3 Loss of Excitation (LOE) Relay Mis-operation

In power systems, the synchronism between generators is maintained by their magnetic fields. The excitation system of a generator is responsible to provide the required energy for the magnetizing reactance. The excitation system also affects the amount of reactive power that the generator produces or absorbs. Changing the excitation current changes the reactive power output of generators that in extreme cases may result in loss of synchronism of the generator. Different types of faults such as field short circuit, field open circuit, accidental tripping of the field breaker, or voltage regulation system failure may lead to the loss of excitation which may consequently lead to loss of synchronism of power generators [14].

Generally the generator terminal impedance can be described based on its output active and reactive power as follows:

$$Z = R + jX = \frac{V^2}{S^*} = \frac{V^2}{P - jQ} = \frac{V^2 \times P}{P^2 + Q^2} + j\frac{V^2 \times Q}{P^2 + Q^2} \tag{1.4}$$

Where V, S, P and Q are positive sequence voltage, apparent, active and reactive powers of the generator. In the normal operating condition, the generator injects active and reactive powers to the system thus R and X are positive and the terminal impedance is located in the first quadrant in the R-X plane. During the loss of excitation, the generators starts to draw reactive power form the power grid and X in Eq. (34) becomes negative. Consequently, the terminal impedance enters into the fourth quadrant in the R-X plane and the endpoint of terminal impedance ranges between the direct axis transient and synchronous reactances. Thus, to protect generators from loss of excitation, conventionally an impedance type relay is utilized at the terminal of synchronous generators. Mason proposed the one negative-offset mho element in 1949 [15]. In order to increase the security of this relay against stable power swing, another negative-offset characteristic with two protective zones was developed by Berdy in 1975 [16]. In this method, negative offset-mho characteristics are defined based on the system condition. The impedance circles diameters are equal to 1.0 p.u. for Zone 1 and X_d (generator synchronous reactance) for zone 2. The downward offset of the zones is equal to half of the generator transient reactance ($X'_d/2$) [17].The typical time delay of LOE is 3 to 5 cycles (0.1 s) for zone 1, and 30- 45 cycles (0.5- 0.75 s) for zone 2.
The impedance trajectory in the power swing condition may enter and leave the mho impedance zone of LOE characteristic in short period of time in comparison to the time for the loss of field condition [18].The impedance seen by the LOE relay traverses into the third quadrant on the R-X plane. The relay in this condition may undesirably detect loss of excitation or loss of synchronism

and mis-trips [16], [19]. The LOE relay characteristic and impedance loci during swing condition are shown in Figure 1.3.

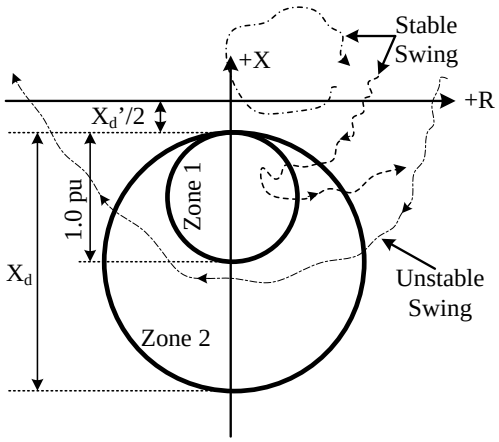

Figure 1.3 Loss of excitation characteristic and impedance loci during stable & unstable swing

In the next chapter the transient simulation (CAPE-PSS/E) platform is utilized to study the mis-operation conditions of the conventional distance and LOE relays.

2. Protection Dynamic Study Circumstance

2.1 Transient relay testing Interface

After recent blackouts in the United States like September 2011, and August 2003 disturbances, studying the protective relay responses on the dynamic behavior of the system becomes essential for the operators in the bulk power systems. In contrast to steady state methods, testing relays in transient conditions provides more realistic testing scenarios to study the response of protective relays during transient condition [10]. In this project, co-simulating platform, CAPE- Transient stability (TS) is used for this purpose. The relay models are implemented in CAPE (computer-aided protection engineering) software which is internally connected to the dynamic model in Siemens-PTI's PSS®E (power system simulator for engineering) software. The integration is carried out in a closed-loop and seamless scheme. The two-sided interface between PSS/E and CAPE is shown in Figure 2.1.

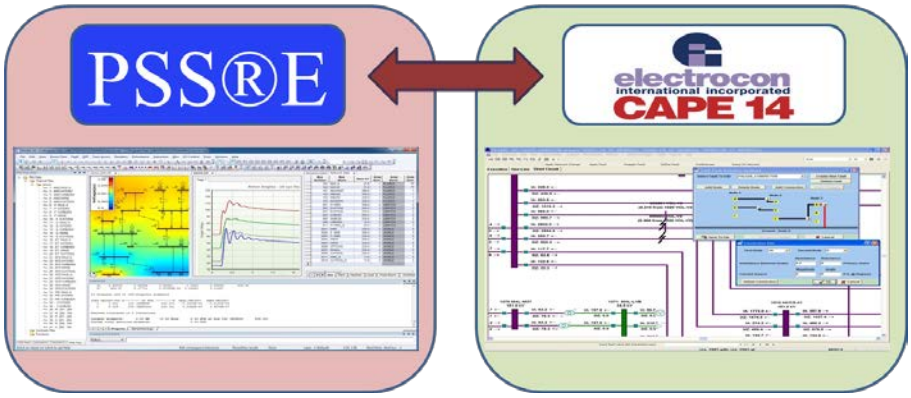

Figure 2.1 Integration between transient model and protection model

1. Description of PSS/E model

For performing the transient study in this project, professional software package PSS/E is internally utilized by the CAPE-TS module of the CAPE software. The basic functions of power system performance simulation work are handled by this computer program; some of the important ones are namely:

- Power flow: this module is basic toll and it is powerful ads easy to use for basic power flow network analysis. Besides analysis tool this module is also used for data handling, updating and manipulation. The Figure 2.3 show the network topology and Newton-Raphson power flow output result of the two-area power system test system. As it is written, the PF converged in 4 iterations.

- Optimal power flow: PSS/E optimal power flow (PSS/E OPF) is a strong toolbox that goes beyond traditional load flow analysis to fully optimize and refine a transmission system.

The final result is the globally optimal solution which simultaneously satisfies system limits and minimizes costs or maximizes the performance.

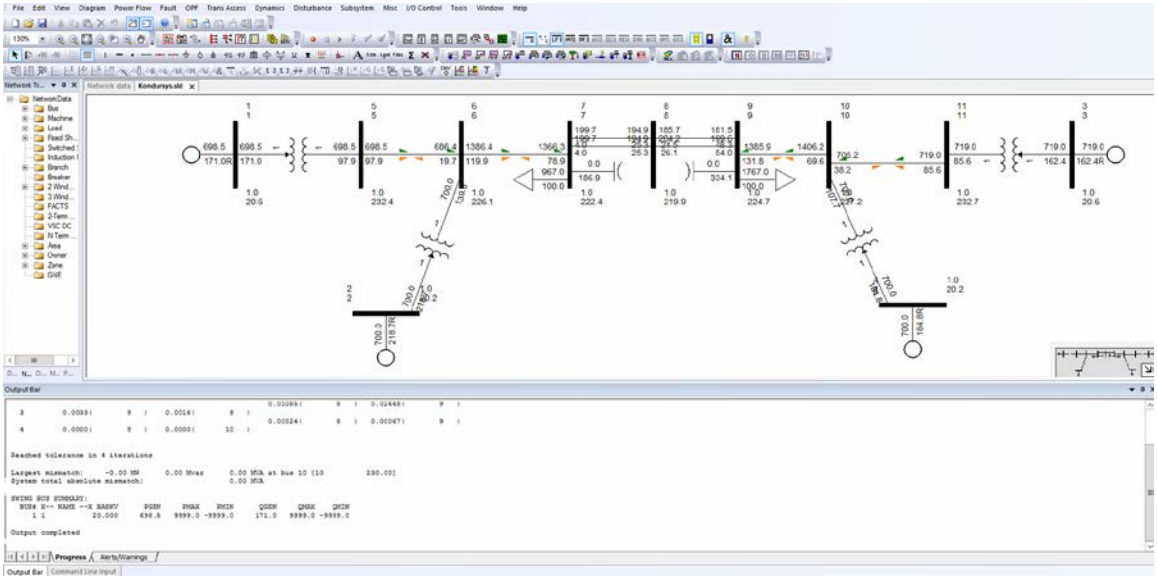

Figure 2.2 PSS/E model graphical interface

- Fault analysis: the PSS/E fault analysis program is fully integrated with the power flow tool. The balanced and unbalanced faults can be studied with this program.
- Dynamic simulations: PSS/E can model system disturbances such as faults, generator tripping, motor starting and loss of field. This program contains an extensive library of generator, exciter, governor and stabilizer models. It also has protection library including underfrequency, distance and overcurrent relays (Its protection library is limited in comparison to the CAPE relay library.).
- Equivalent construction: the large-scale networks can be modeled into internal and external areas to make the analysis easier. This module keeps the study area (internal area) in details and compress rest of the system into an equivalent model.

Since the 1976, the PSS/E program has become one of the most comprehensive, technically advanced and widely used commercial programs in the market. This program employs the updated techniques and numerical algorithms to efficiently solve large scale networks and data [20].

2. Description of CAPE-TS link

PSS/E has relay library but it is not completed, thus the protection system cannot be modeled in details and realistic, so CAPE as one of the well-known protection program is utilized to model the protective relays and devices and simulate their dynamic responses precisely. There is a CAPE-TS module utilizes the PSS/E for transient simulation. Its mean features are:

- Bulk power system can be modeled with thousands of the relays (distance, overcurrent, out-of-step, frequency, voltage, V/Hz, etc.) that have realistic settings.

- The planning and protection models are simulated together so that the interdependence between system dynamics and relay actions can be captured and cascading failures can be studied.
- The transient stability model is studied based on the relay operation in reality.
- Different contingencies and scenarios which may lead to cascading outages can be simulated and the appropriate calibrations can be defined in this platform to prevent those events.
- Different remedial action schemes (special protection schemes) and their associated wide-area control methods can be tested in this platform.

2.1.1 Building the co-simulation platform

Some preliminary data requirements must be prepared prior the transient relay testing, such as [21]:

- *CAPE database file (.gdb)*: This file contains the accurate network data including the sequence data, the protection model and the relays' settings and coordination schemes.
- *PSS/E load flow case (.sav)*: The power flow model of the network is stored in this file.
- *PSS/E dynamic snapshot file (.snp)*: Positive sequence steady-state condition of the system is stored in this file. The faults and disturbances are simulated by applying changes in this file. Based on the fault type, extra nodes are added to the dynamic model of system at pre-specified fault location.
- *Bus and Branch mapping files (.bme & .brm)*: The mappings between buses and branches of the dynamic model (PSS/E) and protection model (CAPE) are established in these files. Dynamic and protection paltforms internally connected to each other through these files during simulation. At each time step, the network topology and configuration are updated in these files after any status change in the protection system model.

In every simulation step, the positive-sequence voltage profile is updated in the transient stability program (PSS/E) and is passed to the protection model (CAPE). Depending on the type of fault (balanced or unbalanced), one or more sequence networks will be used in the fault analysis.

1. Balanced contingency

During the balanced contingency, currents seen by the protective relays are computed by dividing the obtained positive-sequence voltage differences between two ends of the relay line over the line impedance, as follows:

$$I_{\mathrm{Re}lay} = \frac{V_{i1} - V_{j1}}{Z_{Line}} \tag{2.1}$$

Where V_{i1}, V_{j1} and Z_{Line} are the positive sequence voltages at two ends of the line buses and line impedance, respectively.

2. Unbalanced contingency

In the unbalance fault scenario, the fault type and fault location are known. The positive sequence fault current (I_{F1}) can be calculated from the known positive sequence voltages of all neighboring buses of faulted line obtained from the dynamic simulation. Positive, negative and zero sequence circuits are connected together depending on the type of the fault. Then, the negative and zero sequence fault currents (I_{F2}, and I_{F0}) are calculated from the calculated positive sequence current (I_{F1}). For instance, for a single-line-ground fault, three sequence networks are connected in series, so the positive, negative and zero sequence fault currents are equals (I_{F1}=I_{F2}= I_{F0}). The phase currents (I_{af}, I_{bf}, and I_{cf}) at fault location are calculated from the sequence fault currents. Furthermore, the negative and zero sequence voltages at all buses in the protection model are calculated as follows:

$$Y_{BUS} \times \Delta V = I_F \tag{2.2}$$

Where I_F is the fault current at faulted node (zero at all non-faulted buses), Y_{BUS} is the nodal admittance matrix of the faulted network, ΔV is the vector of voltage variation from pre-fault to fault at all buses ($\Delta V = V_{fault} - V_{prefault}$). Since pre-fault negative and zero sequence voltages are assumed to be zero in this calculation, the negative and zero sequence of ΔV are equal to the post-fault negative and zero sequence voltages. The phase voltages (V_{ABC}) of the entire network are calculated from the sequence voltages. The relay currents are then calculated based on the computed voltages and the network impedances. Relays operate based on these calculated currents [21].

Once the phase currents are determined, the operation of protective relays and statuses of breakers are evaluated in the protection model (CAPE). If any of protective devices operates, the network topology in dynamic and protection models is updated simultaneously. In the next iteration, PSS/E calculates the new voltage profile in the new network configuration and passes to CAPE. The CAPE-TS co-simulation procedure is depicted in Figure 2.3.

2.2 Single Machine Infinite Bus System Simulation Results

A single machine infinite bus (SMIB) system is used to study the conventional transmission line distance and LOE relays' performance and mis-operation condition during the power swing phenomenon. The system shown in Figure 2.4, is simulated using CAPE-PSS/E platform. In PSS/E, the sending bus (bus 1) is modelled as a synchronous machine with dynamic model of GENROU type. This model is based on the swing equations for cylindrical rotor generators. The excitation system is modelled as IEEE ESST1A. The receiving end (slack bus) is modelled by the classical generator model, GENCLS. The test system data are given in the Appendix [22]. Prior to fault occurrence the phase angle difference is δ=20 degrees.

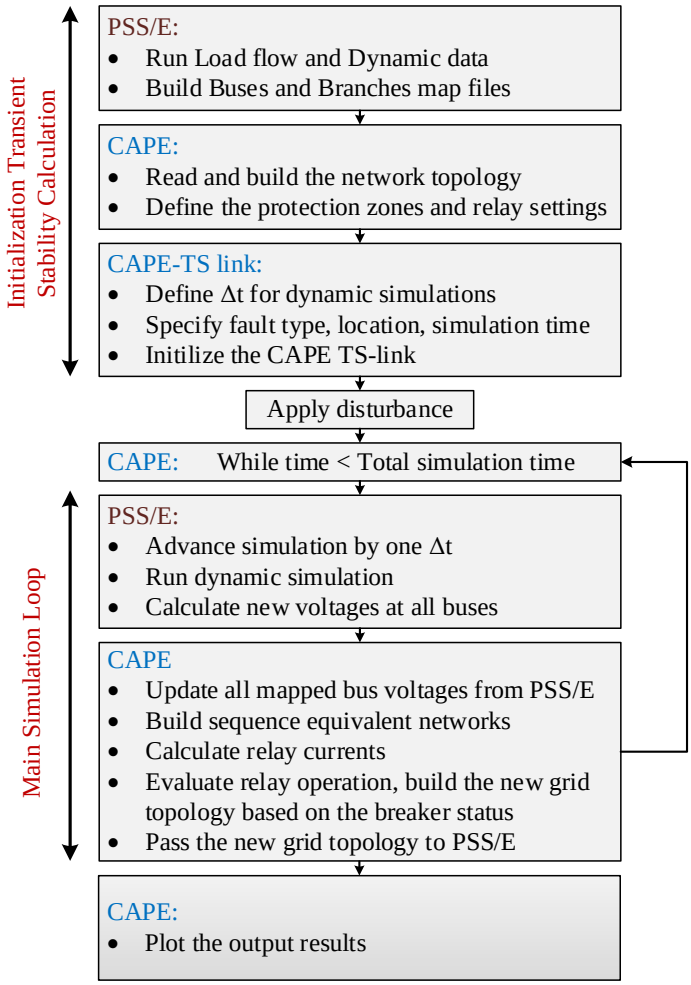

Figure 2.3 CAPE-TS co-simulation flowchart.

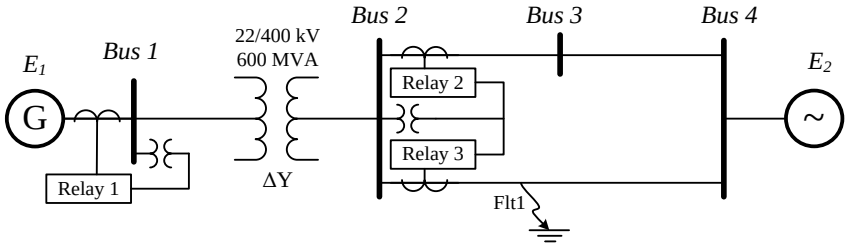

Figure 2.4 One line diagram for SMIB system.

Three protective relays are defined in the system. It is assumed two line protective relays (SEL-321 type) cover line 2-3 (Relay#2) and line 2-4 (Relay#3) and one relay (SEL-300G type) is protecting generator#1 (Relay#1) from LOE. The zone 1 and zone 2 of the transmission line distance relays are set %80 and %120 of the forward line impedance respectively. Typically, zone 1 trips without time delay while zone 2 has a time delay of 20- 30 cycles or (0.3–0.5 s) [23]. For

relay#2 which its response during power swing condition is studied, the quadrilateral inner and outer blinders are set according to section 1.2. The inner radius and outer radius are 65° and 45°, respectively. The blocking timer is set with the typical delay 2 cycles [11]. The LOE relay characteristic is set based on conventional two zone scheme. The designed mho characteristics of the installed relays are depicted in Figure 2.5.

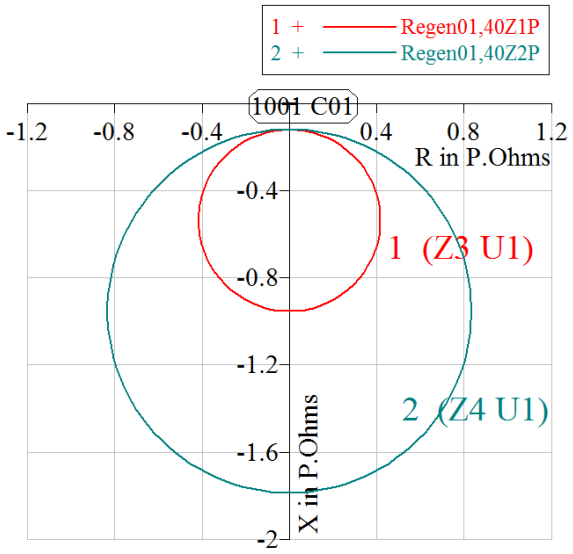

(a)

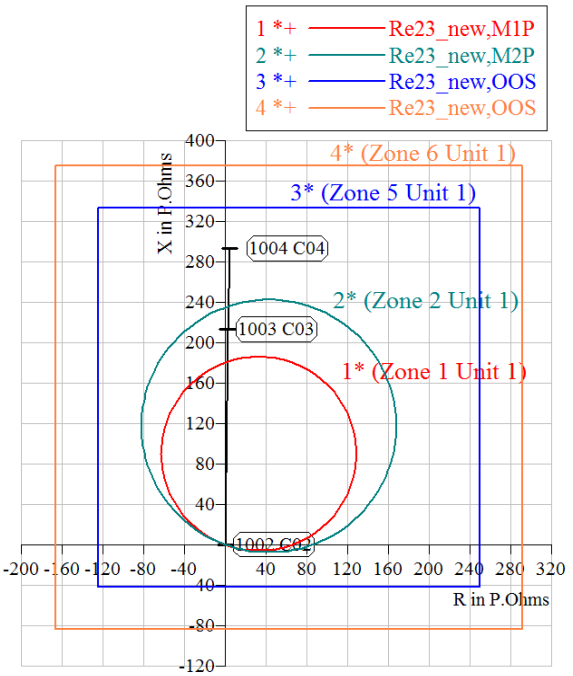

(b)

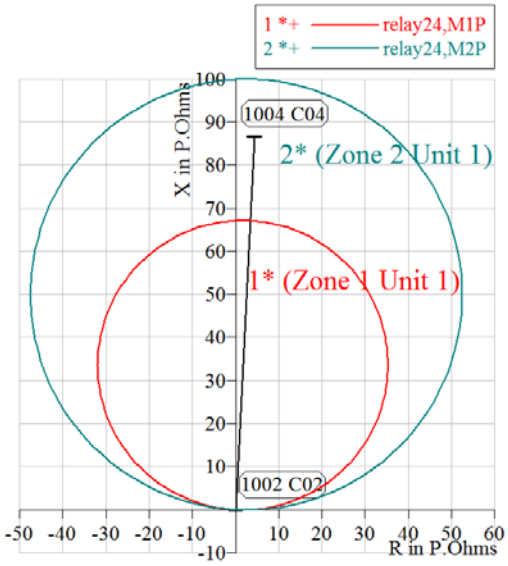

(c)

Figure 2.5 Designed mho characteristic of distance elements

(a) Relay#1 (SEL 300G- LOE relay), (b) Relay#2 (SEL321- Distance relay), and (c) Relay#3 (SEL321- Distance relay)

Once the protection scheme of the test system, which includes three relays as explained above, is defined, the responses of the relays to faults are studied. Then, some scenarios under which the relays mis-operate are discussed.

To study the response of the LOE relay to a fault in the excitation of the machine#1, a short circuit is applied to the excitation system of generator#1 at 0.3 s. The impedance trajectory in LOE condition is shown in Figure 2.6. The apparent impedance trajectory traverses toward the mho characteristic of the relay and enters zone 2 of the LOE relay at 1.37 s, afterwards, it enters smaller zone of the LOE relay. The pre-determined time delay for the zone 2 of the LOE relay expires after 0.65 s, then the breakers operate after 0.05 s delay, so the fault is cleared at 2.07 s by disconnecting the generator form the rest of the grid.

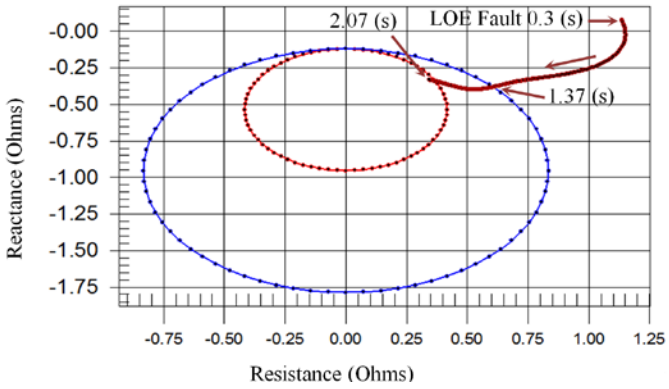

Figure 2.6 Apparent impedance loci and relay#1 operation during Loss of Excitation condition

In the next step, different fault scenarios are applied to the system and operation of the protective relays during stable swing cycles are studied. Some of the scenarios that lead to relay operations are summarized in Table 2.1.

Table 2.1 Operation scenarios of protective relays during stable power swing condition

Scenario No.	Mis-operated Relay	Operated element and condition	Fault clearing time (s)	PSB time delay (cycle)	Zone 2 Time delay (cycle)	Impedance trajectory inside relay zone2	
						Entrance Time (s)	Exit/ Trip Time (s)
1	Distance Relay 2	PSB Mis_operated	0.15	2	24	0.6	Trip (1.075 s)
2	Distance Relay 2	PSB Blocked	0.15	1.2	24	0.6	Exit (1.66 s)
3	LOE Relay	Zone 2 Mis_operated	0.49	—	<49	0.65	Trip (1.46 s)

2.2.1 Distance relay response

To study the response of distance relays during post fault conditions, a 3-phase fault is applied at 0.1 s in the zone 1 of protective relay#3 on the middle of the line between buses 2 and 4 (fault is shown as *Flt1* in Figure 2.4). The fault is detected instantaneously by the relay and cleared after breaker operation delay 3 cycles at 0.15 s. The post fault system experiences stable power swing condition.

Rotor angle of Machine#1 and impedance locus trajectory at distance relay#2 during the stable swing are depicted in Figure 2.7. The apparent impedance loci moves towards the relay (SEl-321) characteristics.

At first, it enters the blinders characteristic curves and then moves into the protection zones of the relays. The apparent impedance passes the distance between outer and inner characteristics in ΔT_B= 1.43 cycles (i.e. the period between 0.385 s to 0.409 s). In the first case study (scenario 1) the PSB

timer is set to 2 cycles, since it is larger than the time interval that impedance loci moves between the blinders (ΔT_B), the PSB element mis-operates and detects this condition as the fault, so the zones 1 and 2 are not blocked.

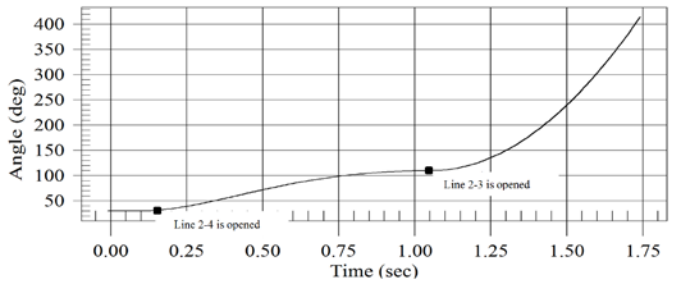

(a)

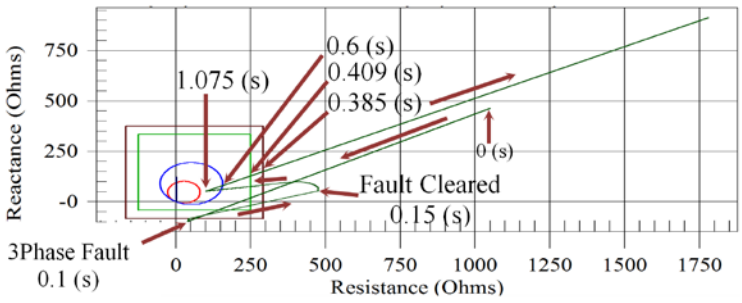

(b)

Figure 2.7 Relay#2 performance during stable swing- Scenario 1

(a) Angle swing of the system, and (b) Apparent impedance loci trajectory

During the stable post fault condition, the impedance trajectory enters the zone 2 at 0.6 s and after pre-defined zone 2 time delay (24 cycles), the unblocked relay# 2 mis-operates and detects the stable power swing condition as a fault. Then, the breaker operates after a time delay (3 cycles) and disconnects the protected line at 1.075 s (shown in Figure 2.7.b).

If the PSB delay of relay#2 is set to 1.2 cycles which is less than the ΔT_B, the blocking element operates correctly and blocks the mho characteristics. The rotor angle of Machine#1 and impedance locus trajectory at relay#2 during the stable swing are depicted in Figure 2.8. During the stable post fault condition, the impedance trajectory enters the zone 2 at 0.6 s and leaves the zone 2 at 1.66 s. the period which the apparent impedance traverses inside the zone 2 longer than the set zone 2 time delay (typically $t_{setting\_Z2}$= 24 cycles) but the PSB element blocks the relay correctly.

2.2.2 Loss of excitation relay response

To demonstrate scenarios that may lead to mis-operation of LOE relays, the electrical center should be located in generator's protection zone. Therefore, the line impedance values of the network shown in Figure 2.4 are reduced to the two third of the previous

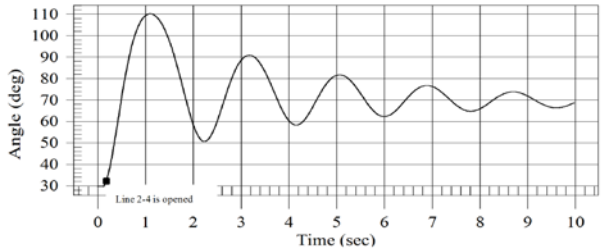

(a)

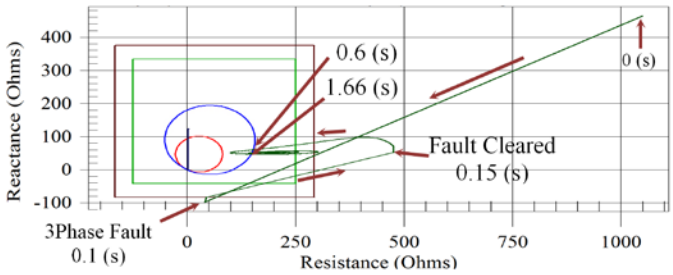

(b)

Figure 2.8 Relay 2 performance during stable swing- Scenario 2

(a) Angle swing of the system, and (b) Apparent impedance loci trajectory

cases. In this condition, the electrical center of the system moves toward the synchronous machine impedance value and the protective relay of generator may mis-operate during power swing. A 3-phase fault is applied on line 2-4 at 0.1 s and relay#3 clears the fault in zone 2 after the set time delay at 0.49 s. This condition causes stable power swing in the system. The rotor angle of machine# 1 and impedance locus trajectory at LOE relay location during the stable power swing are depicted in Figure 2.9.

During the first power swing, apparent impedance trajectory enters zone 2 of the LOE relay at 0.65 s, then moves slowly inside the protection zone, and exits zone 2 at 1.46 s. Since the typical time delay of LOE is 3 to 5 cycles (0.1 s) for zone 1, and 30- 45 cycles (0.5- 0.75 s) for zone 2 [17], relay#1 with these typical time delays that are smaller than the time interval that the impedance locus traverses into mho characteristics ($t_{setting\_Z2}$ < 0.81 s) mis-operates and detects the stable power swing as a fault and issues trip command.

2.3 WECC System Co-simulation

In this section, WECC data, representing the heavy load in summer (HS) 2016, is used to study

the dynamic performance of the protective relays. All the generators are equipped with a turbine governor, exciter, and PSS. The total active generation is 207358 MW in this case. WECC system has different areas, which are connected with strong tie lines. Moreover, the distance relays (SEL-321) are modeled in details in the protection platform based on the typical settings which were explained in pervious section. The inter ties over 100 kV between different areas of WECC system are shown in the Figure 2.10 [24].There are three intertie lines (500 kV) between Oregon and California. The California- Oregon Interties (COI) transfers more than 4800 MW from north to south in this peak load case.

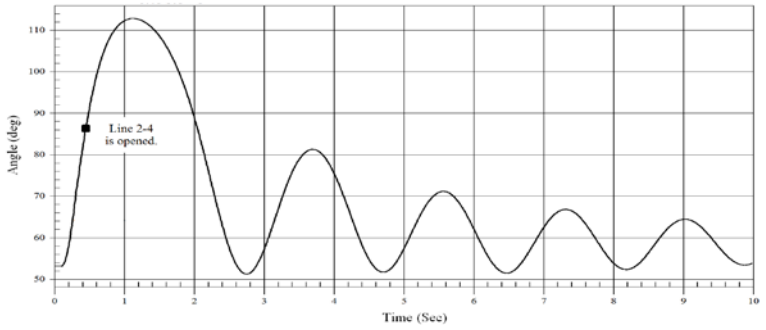

(a)

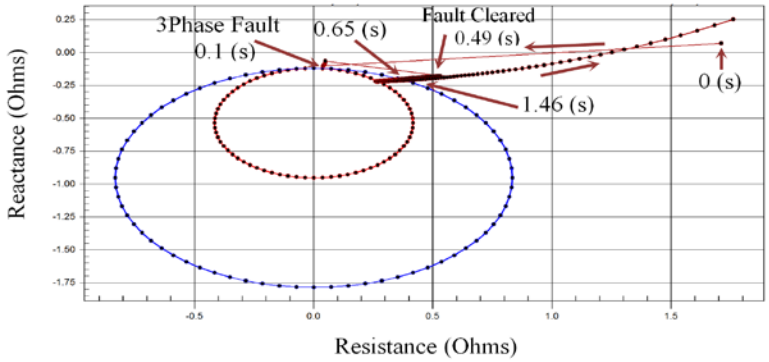

(b)

Figure 2.9 Generator 1 relay performance during stable swing- Scenario 3

(a) Angle swing of the system, and (b) Behavior of LOE relay during stable swing

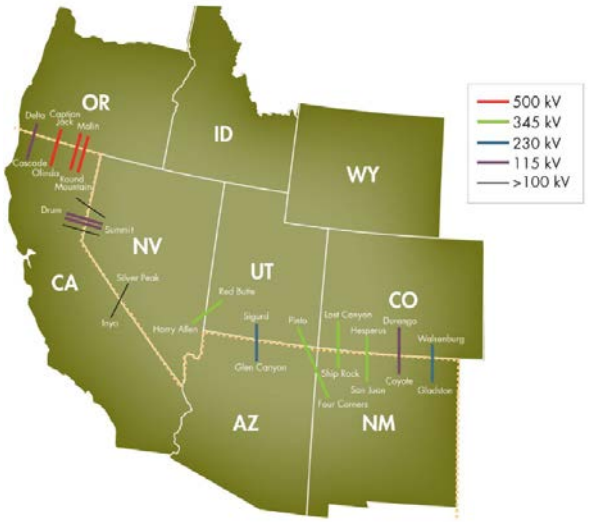

Figure 2.10 Interties between WECC areas (over 100 kV) [24]

The investigated reports on the WECC system described the extreme contingencies as combination of events which are followed by actions of protective relays and RAS devices [25]. Since the COI are the major transmission lines in the WECC system, any events on them causes sever swing condition for the system. The COI tie lines are shown in the Figure 2.11. Two 500 kV lines are paralleled between Malin and Round Mountain substations and the last one is between Captian Jack and Olinda substaions.

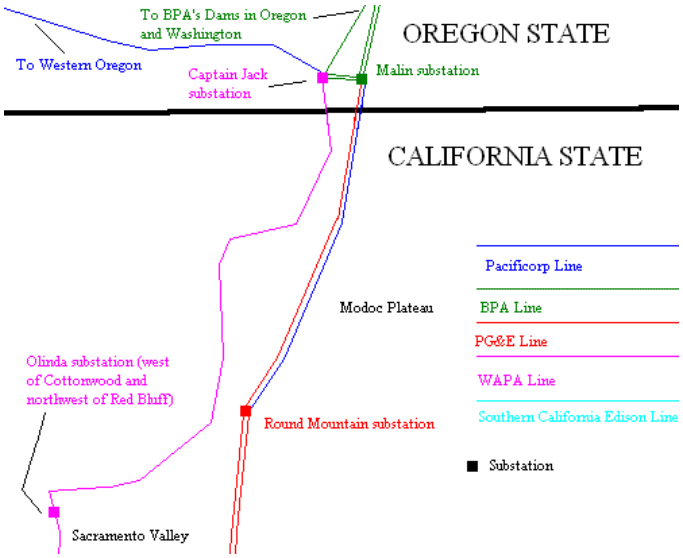

Figure 2.11 Marginal substations of COI interties [24]

In the next step, different fault scenarios are applied to the system and operation of the protective relays during swing cycles are studied. However, two types of outages which occur at the COI lead to critical contingencies in the WECC, such as follows [25]:

2.3.1 Stable Swing Condition

A 3-phase fault on the marginal bus# 40687 (Malin substaion), located in the Northwest area (area#40) is applied at 0.1 s. This contingency is cleared at 0.15 s (after 3 cycles, time delay of the breakers) by tripping all the connected lines to this bus included two parallel COI tie lines connected to the Malin substation. This sever double line outage (SDLO) initiates a stable power swing. The tielines configuration between PG&E and northwest areas and the marginal substaions are shown in Figure 2.12. The relative angles of the generators in area#30 (PG&E) and area#40 (Northwest area) are shown in the Figure 2.13. All the generators rotate as a coherent group. In the stable swing, none of the distance relays mis-operated.

2.3.2 Unstable Swing Condition

If a fault occurs on the bus#45035 Captain Jack in area#40 (Northwest area) at 0.1 s and cleared by disconnecting all the connected lines to this bus at 0.15 s. So all the three 500 kV tie-lines will be tripped because of overloading. Losing the strong transmission paths causes large mismatch between load and supply in the system. Therefore the generators start to oscillate and split in two separate groups. The generators in the northern part of the COI lose their synchronism and accelerate in comparison to the generators located in the southern part (California).

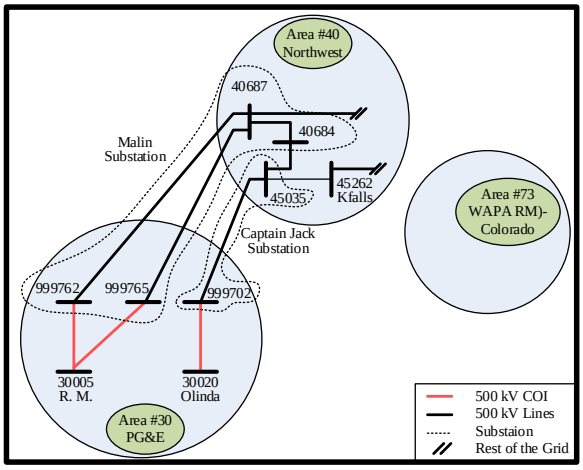

Figure 2.12 Marginal substations of COI interties

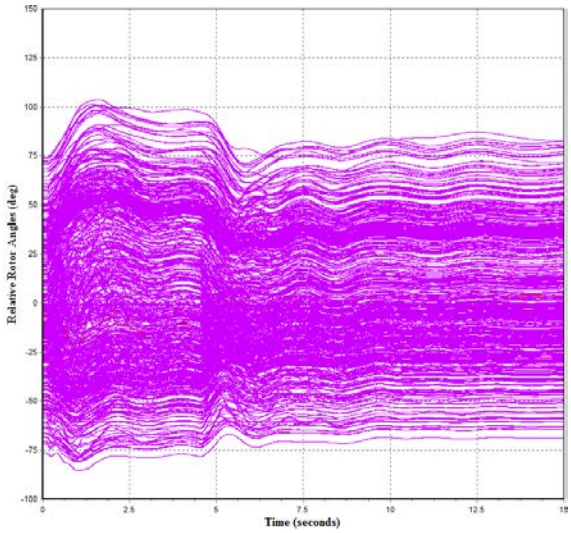

Figure 2.13 Generators relative rotor angles in the stable swing period

This triple line outage (TLO) leads to an unstable swing oscillation. The rotor angles of generators are shown in Figure 2.14. In such situation, there is a event-based operation of remedial action schemes (RAS) to protect the system from cascading events [26]. One of the significant actions for this outage is northeast/southeast separation (Ne/SE separation) strategy that provides controlled separation within the WECC system along the predetermined branch groups [24]. The severe outages are summarized in

Table 2.2.

Table 2.2 Extreme contingencies in wecc System

Scenarios	**Operating Conditions**	**Contingency Locations**	**Outage**	**Swing Condition**
Case#1	HS	COI	SDLO	Stable
Case#2	HS	COI	TLO	Unstable

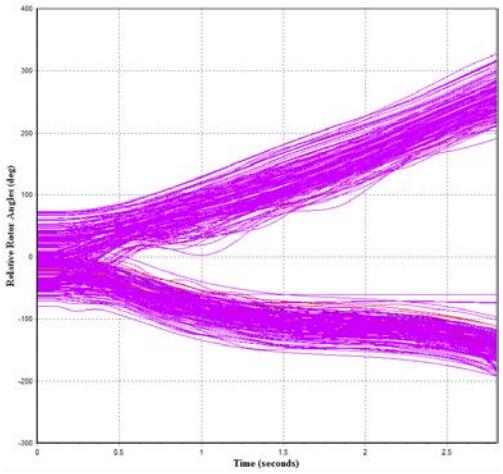

Figure 2.14 Generators relative rotor angles in the unstable swing cycle

During the unstable condition, some of the distance relays in the area#73 WAPA RM (Western Area Power Administration Rocky Mountain-Colorado shown in Figure 2.12) on the eastern part of WECC network mis-operate.

Distance relays are modeled to protect %80 and %120 of the line in zone 1 and zone 2. The zone 1 operates simultaneously, and the zone 2 has 24 cycles delay, and the blocking time delay is the typical value, 2 cylces (Typical time settings). For instance, two different apparent impedance trajectories are studied on the R-X plane of the distance relays in (WAPA RM).

1. The distance relay on 345 kV Line from bus 79049 (Montrosse) to bus 79072 (Hesperus)

If the OSB is disabled, the apparent impedance enters the zones 2 and 1 of the relay at 2.39 s and 2.58 s. After entering the zone 1, the relay detects the swing condition as a fault and mis-operates by passing 3 cycles (breaker delay), it trips the line at 2.63 s. The impedance trajectory is depicted in Figure 2.15.

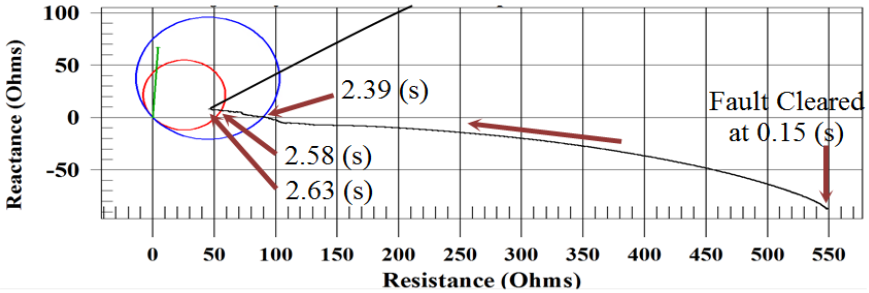

Figure 2.15 Relay mis-operation during unstable swing- Line 79049- 79072

If the OSB is enabled, the impedance enters the outer and inner blinders at 1.79 s and 2.14 s, respectively. Since the time interval between blinders are larger than 2 cycles (OSB typical delay), the relay is blocked. The impedance trajectory with the enabled blinders is shown in Figure 2.16.

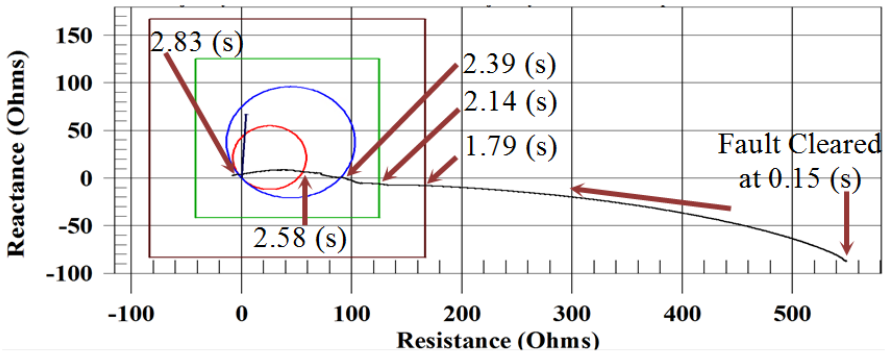

Figure 2.16 Relay blocked during unstable swing- Line 79049- 79072
The distance relay on 230 kV Line from bus 79021 (Curecant) to bus 79045 (Lostcany)

If the OSB is disabled, the apparent impedance enters zones 2 and 1 of the relay at 2.39 s and 2.60 s. After entering zone 1, the relay detects the swing condition as the fault and mis-operates after 4 cycles (breaker delay), it trips the line at 2.67 s. The impedance trajectory with the disabled blinders is shown in Figure 2.17.

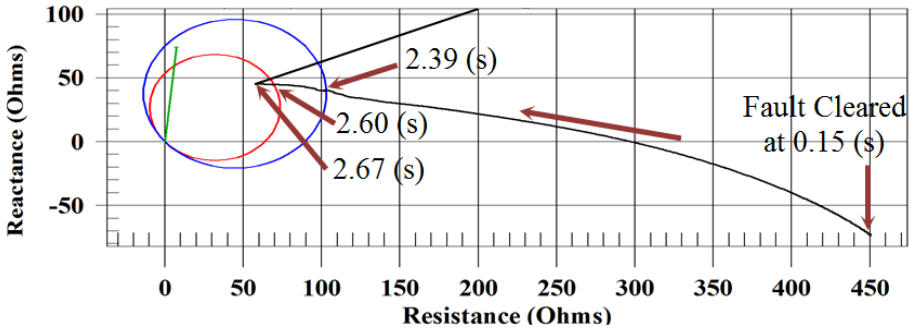

Figure 2.17 Relay mis-operation during unstable swing- Line 79021- 79045

If the OSB is enabled, the impedance enters the outer and inner blinders at 1.82 s and 2.19 s, respectively. Since the time interval between blinders are larger than 2 cycles (OSB typical delay), it is blocked the relay. The impedance trajectory with the enabled blinders is shown in Figure 2.18.

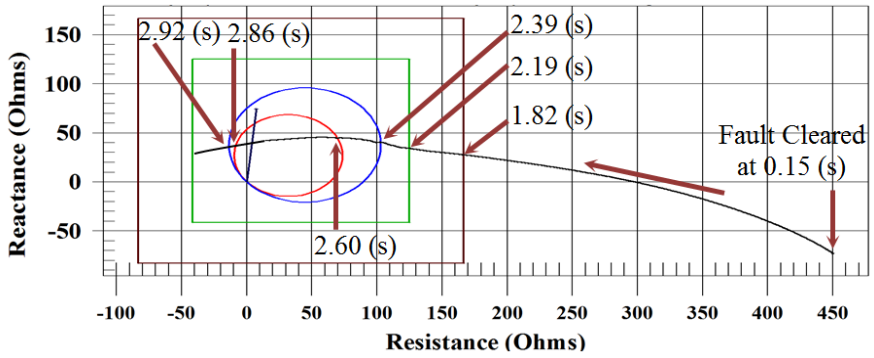

Figure 2.18 Relay blocked during unstable swing- Line 79021- 79045

Malfunction of these distance relays triggers a RAS action (TOT2A) (when the Nucla generators inject power above 60 MW to the grid, the Montrose- Nucla 115 kV line is automatically transfer tripped) [26], and by utilizing the appropriate blocking functions, the specific RAS (TOT2A) is not initiated which can minimize the cascading vulnerability impacts.

3. Power Swing and Fault Detection Methods

In this chapter, different methods that have been proposed for discriminating power swings and fault conditions for distance relay and LOE relay are introduced. Moreover, the new algorithm based on the rate of change of angle is proposed to prevent LOE relay mis-operation and detect the swing condition. Finally, the performance of the proposed technique is tested in the co-simulation platform.

3.1 Power Swing Detection Techniques for Distance Relays

As explained in the first chapter, the power swing blocking scheme is added to the conventional distance relay to detect power swing and prevent relay mis-operation. Traditional methods measure the positive-sequence impedance seen by the relay and the rate of change of impedance. During normal operating conditions the measured impedance is the load impedance and that point is far away from the distance protection zones. When a fault occurs the measured impedance jumps immediately from the load impedance to a point on the impedance plane that represents the fault. On the other hand, when a power swing occurs the measured impedance moves slowly at some trajectory in the impedance plane and at a rate depending on the slip frequency between the machines. This large difference in the speed of movement of impedance in used to differentiate between faults and power swings. Different combinations for impedance measuring elements were proposed for PSB function such as two-blinder scheme, and concentric characteristic scheme [10]. Moreover, a method based on the rates of change of swing center voltage (SCV) was explained in [27]. For instance in a two-source equivalent system when a power swing occurred, due to a slip frequency between the two machines the voltage at the electrical center becomes zero when the angel between two machines are 180 apart. The Figure 3.1 illustrates the voltage phasor diagram of a general two-machine system, with SVC shown as the pahsor from the origin to the O'.

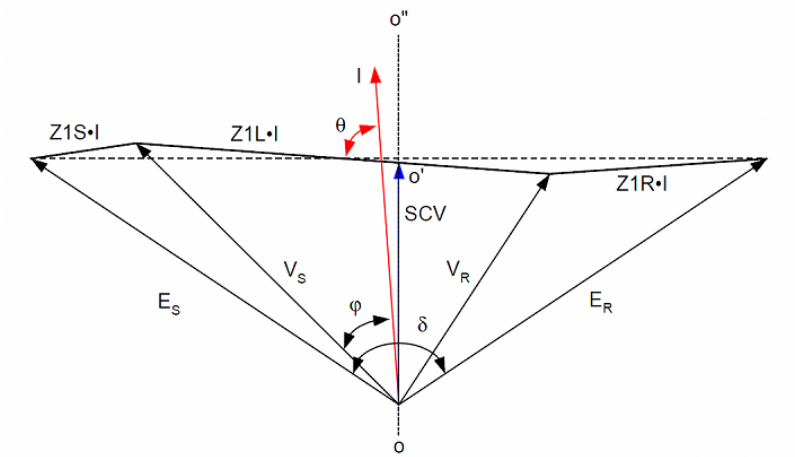

Figure 3.1 Voltage phasor diagram of a two-source system and the relative SVC

The power swing condition is detected when the rate of change of SVC is larger than a threshold. More details of this method is provided in [27]. In [10] the continuous changes of current (ΔI) is

used to detect power swing. If the difference of ΔI value in three consecutive cycles is greater than 5% of the nominal current, the power swing condition is detected.

These methods can easily detect very fast swings but may need to be complemented by conventional rate-of-change-of-impedance method for extremely slow power swings [10]. By utilizing newer technologies such as phasor measurements units and signal processing techniques various methods have been proposed to detect power swing. In the following section one of the non-traditional power swing detection method for distance relays based on the wavelet transform algorithm is explained and simulated results are presented.

3.1.1 Wavelet transform to detect fault condition in distance relay

In [22] a method based on the wavelet transform is introduced to reliably detect power swing as well as detecting symmetrical faults. Wavelet analysis can be used to find abrupt changes in any signals. A wavelet is a waveform of effectively limited duration that has an average value of zero. Wavelet analysis is the breaking up of a signal into shifted and scaled versions of the original (or mother) wavelet. Since the symmetrical fault and power swing signals have different frequency behavior, they can be detectable by extracting the high frequency components from the voltage and current waveforms. There are different mother wavelets, which are used to compare with the original signal. The most used ones are Haar, Daubechies (db), and Morlet.

- Discrete wavelet transform

In this method, the signal is filtered by a high band and low band filters as explained in Fig. 28. The detail coefficients of the each level are defined by the high pass filter (D stages) and the approximated coefficients are calculated by low pass filters (A stages). The wavelet tree is depicted in Figure 3.2.

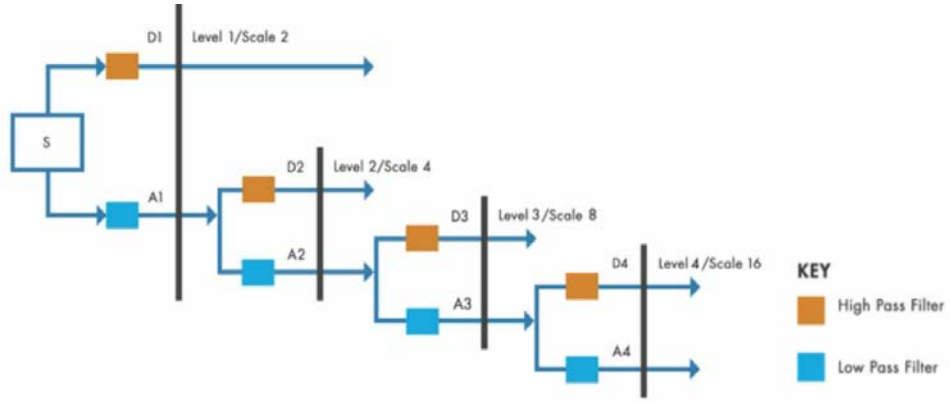

Figure 3.2 Decomposing the data into different coefficients

By this technique the abrupt changes of transient conditions in the voltage, current, and impedance signals can be captured at different levels.

In [22], the level 1 (D1) with mother wavelet Daubechies (db4) is chosen for fault detection from swing. If the changes in the detail coefficients of current and voltage signals are larger than a

threshold, transient condition is detected. By using the D1 coefficient criteria, the out of step blocking function in protective relay can distinguish power swing from fault.

- Simulation results

Single machine infinite bus system is modeled in Matlab Simulink (Figure 3.3). Two different symmetrical faults is studied for detecting the power swing and fault condition.

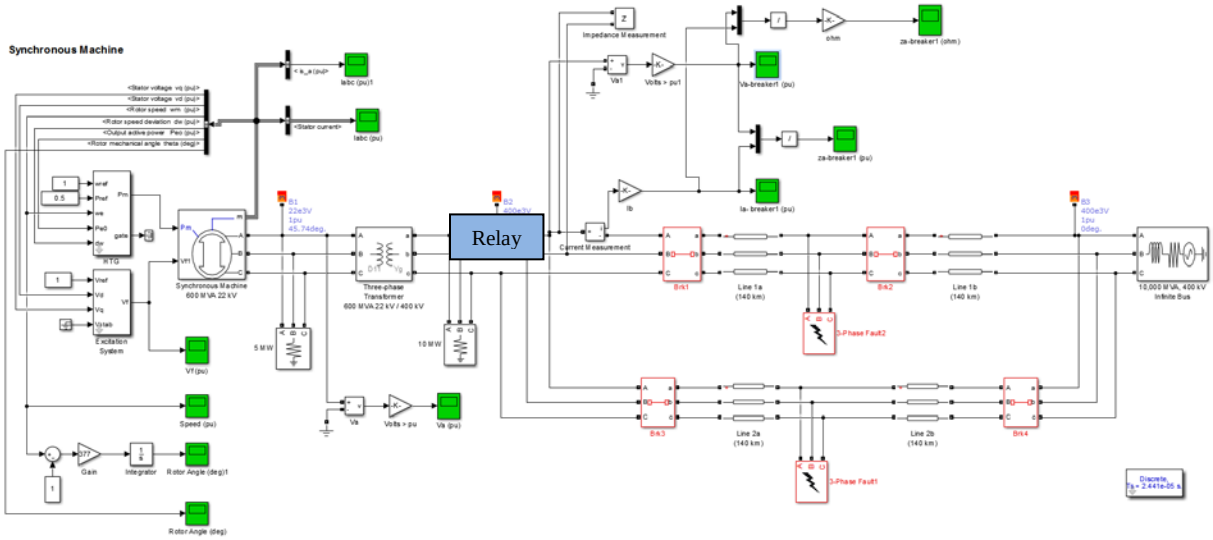

Figure 3.3 Single machine infinite bus system

1. 3-phase fault

A 3-phase to ground fault is applied on the lower line at t=1 s, then breaker#3 and breaker#4 operate and disconnect the line and clear the fault after 5 cycles at t_c=1.1 s. This contingency leads to a stable swing condition.

During the swing cycles, out of step blocking (OSB) function, blocks the distance element of the relay, then if a fault happened in this condition, the relay should detect it and operate. So, a fault on the upper line (fault#2) occurs at 6 s and it is cleared after 0.1 s. The sampling rate is 40.96 kHz in this simulation. Daubechies wavelet db4 is used as the mother wavelet. The wavelet transform is performed in a window length of two cycles (data point in each window N=1365=40.96kHz*2/60). This window moves along the signal as shown in Figure 3.4 and different levels detail coefficients (D) are calculated by decomposing the original signal.

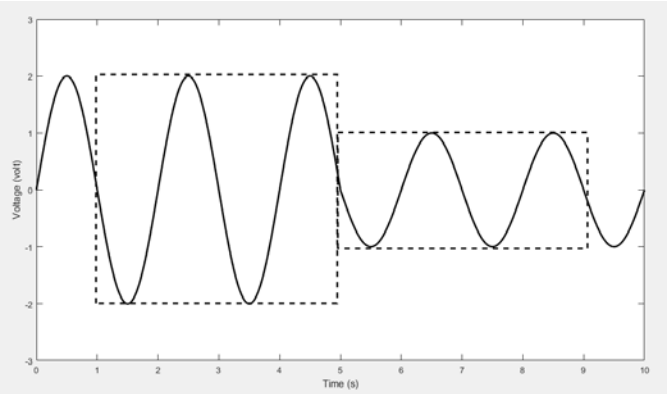

Figure 3.4 Two cycle sampling window

The relay terminal voltage signal and its 4-level detail coefficients are shown in Figure 3.5. As it is clear the detail coefficients are equaled to zero except for the changes inceptions caused by swing or fault conditions. For instance, during the swing, the D1 coefficient variations (in the red rectangle) are between -30 to 30 but in the fault condition (Blue rectangle) this coefficient changes between -90 to 90. The D1 abrupt changes in the rectangles during swing cycle and fault are magnified in Figure 3.6and Figure 3.7, respectively.

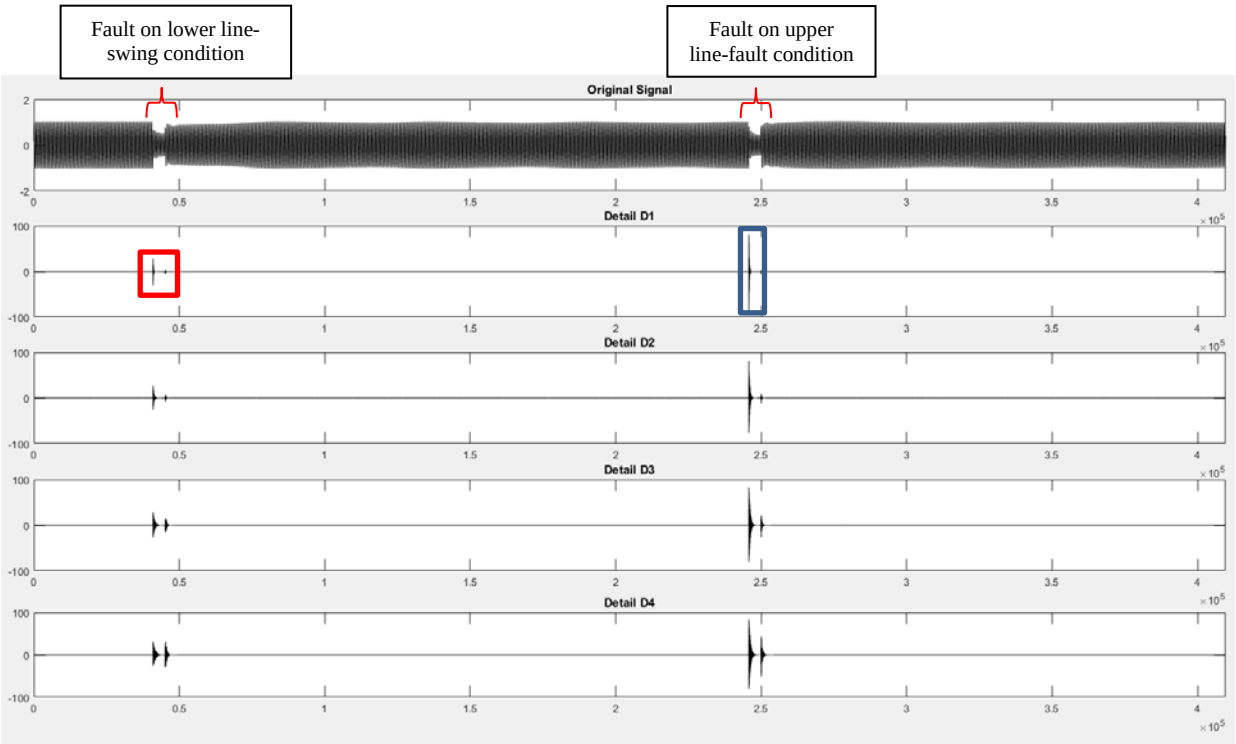

Figure 3.5 Terminal voltage signal and its 4-level detail coefficients

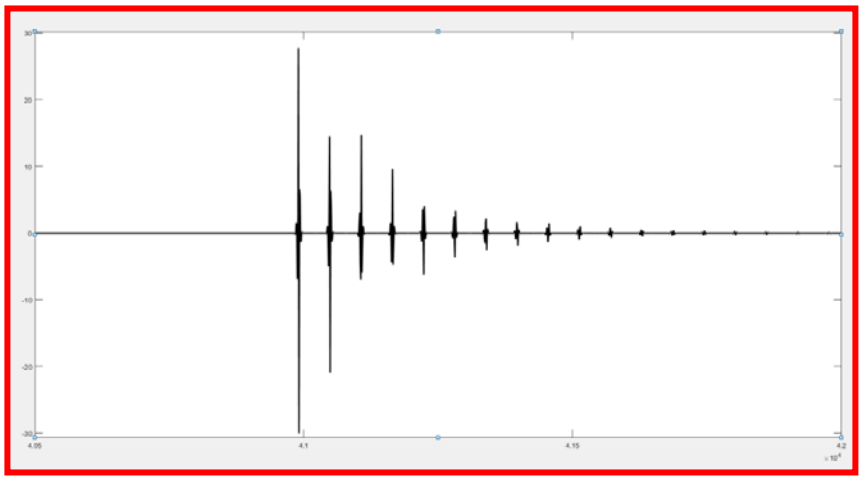

Figure 3.6 D1 variations (voltage signal) during the power swing

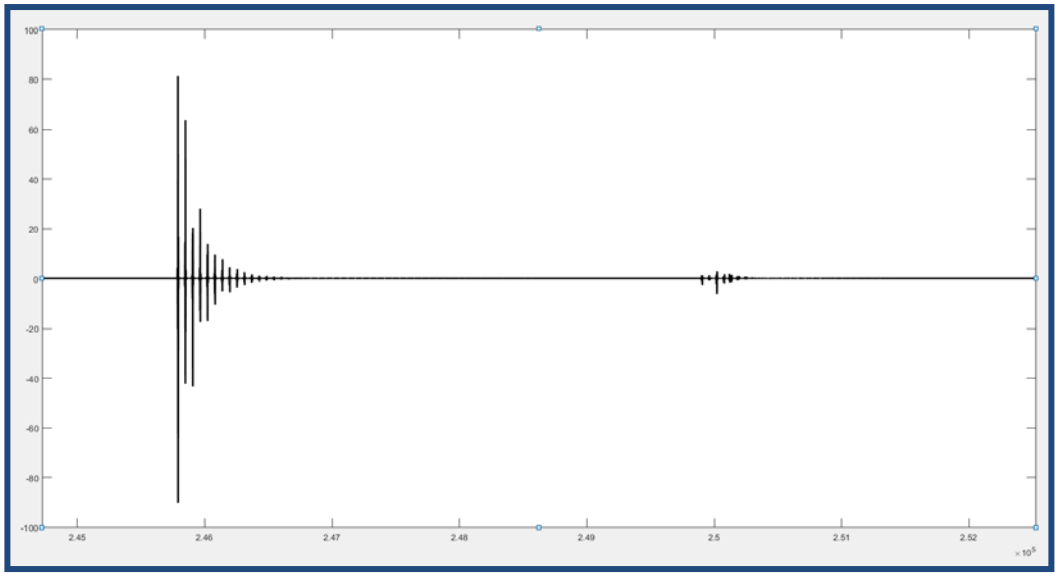

Figure 3.7 D1 variations (voltage signal) during the 3-phase fault

Furthermore, the current at the relay terminal and its 4-level detail coefficients is depicted in Figure 3.8 The detail coefficients are equaled to zero except for the changes inceptions caused by swing or fault conditions. D1 coefficient during the swing (in the red rectangle), is much greater than the one during the fault (Blue rectangle). During the swing they change between -12 to 12 while the changes in the fault are very small. The D1 abrupt changes in the red rectangle during swing cycle is magnified in Figure 3.9.

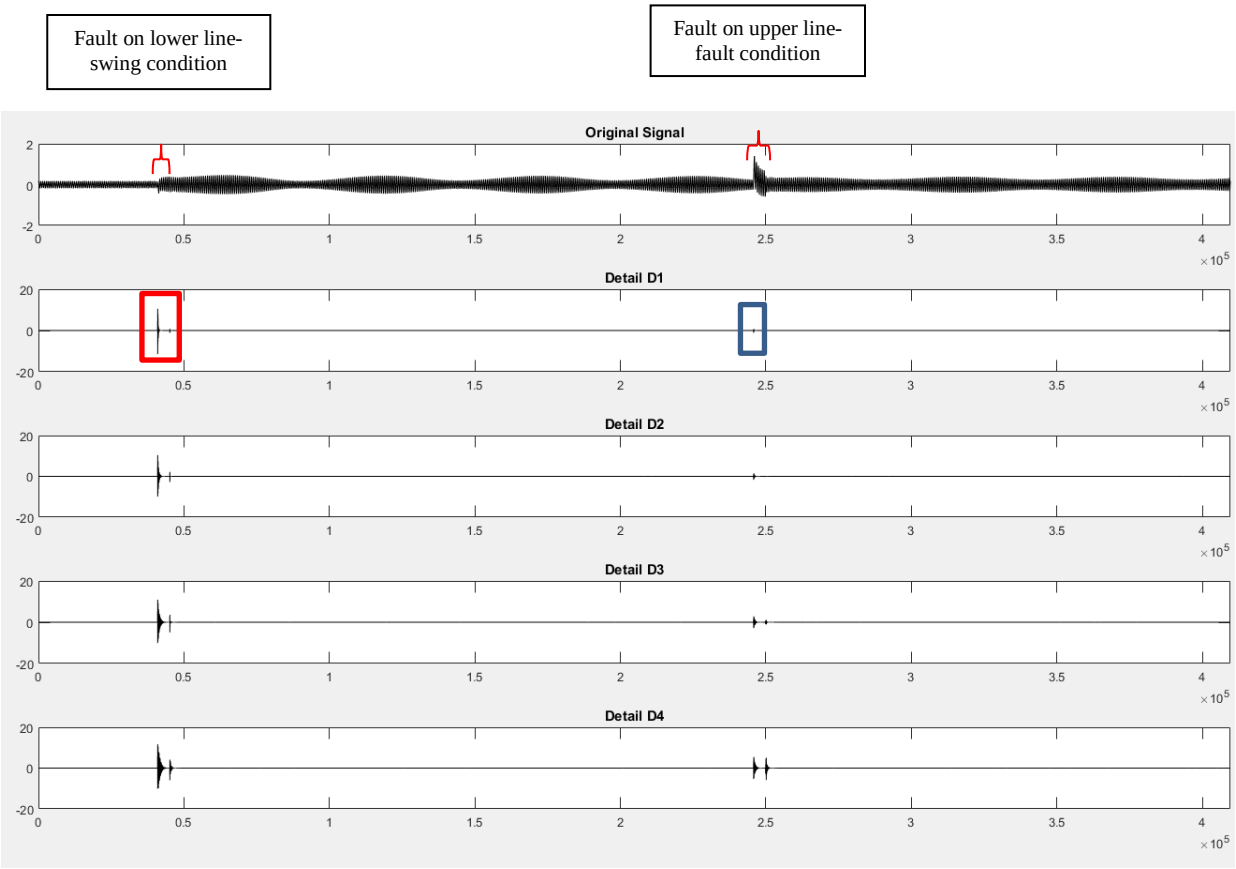

Figure 3.8 Relay terminal current signal and its 4-level detail coefficients

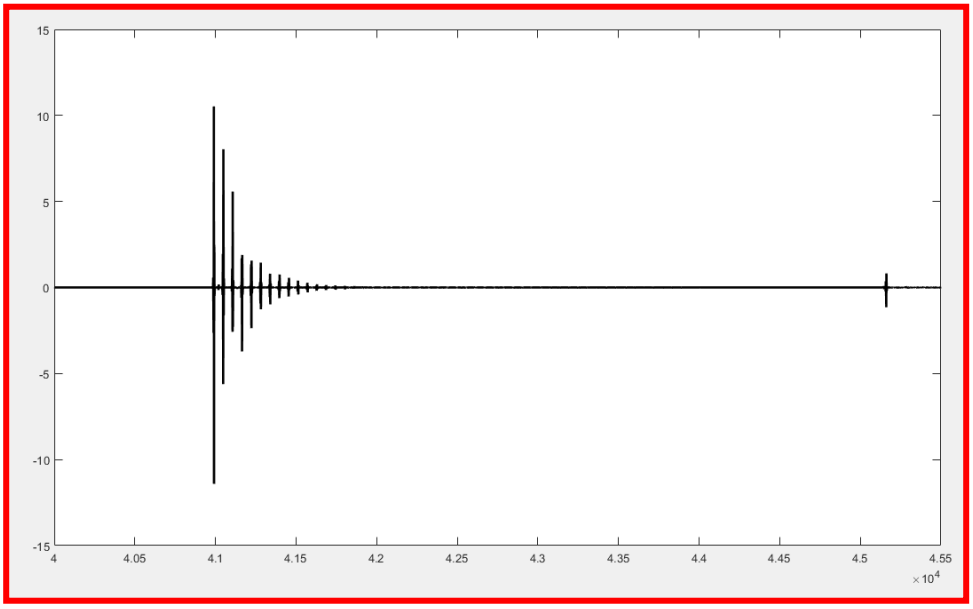

Figure 3.9 D1 variations (current signal) during the power swing

2. Phase to phase fault

Line to line fault is occurred between two phases. The fault between phases A and B is applied with similar location and timing as the pervious case (3-phase fault).

The detail coefficients for voltage and current at the relay location are depicted in Figure 3.10. The D1 abrupt changes in the rectangles during swing cycle and fault are magnified in Figure 3.11 and Figure 3.12, respectively.

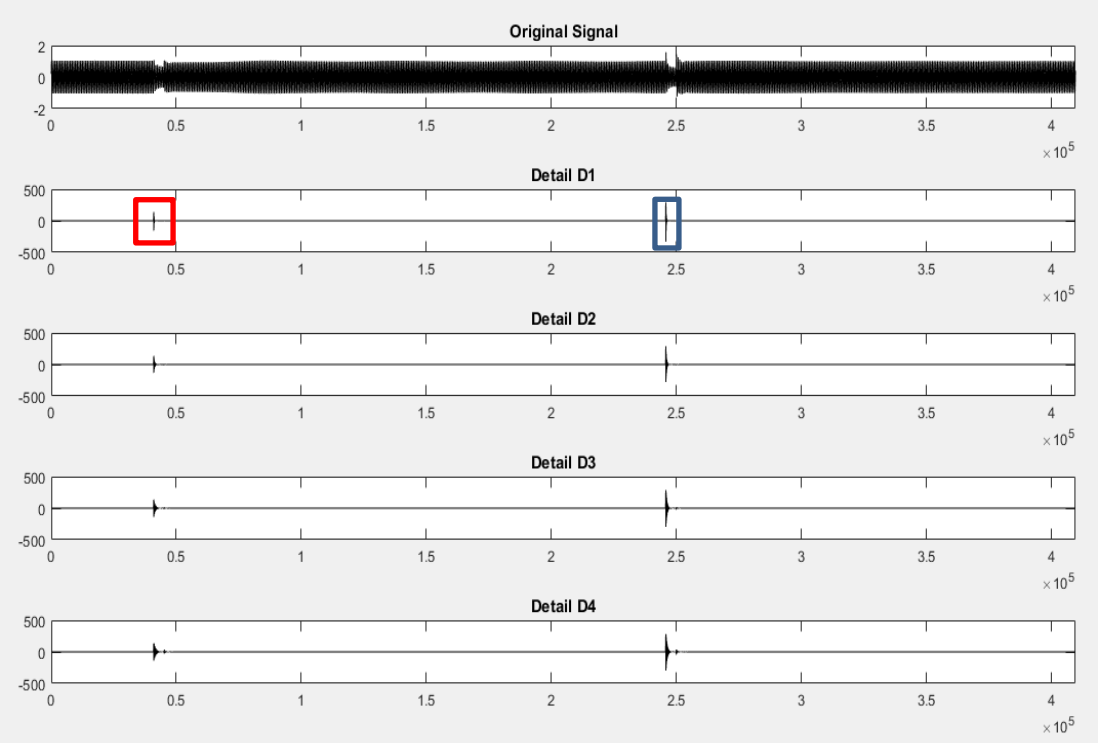

Figure 3.10 Terminal voltage signal of relay and its 4-level detail coefficients- line-line fault

It is obvious, the D1 coefficient in fault condition are larger in comparison to the swing cycle. By choosing an appropriate threshold for D1 coefficient of the voltage the relay can distinguish fault from swing. If the D1 coefficient of voltage is larger than the threshold, the relay should operate for the fault.

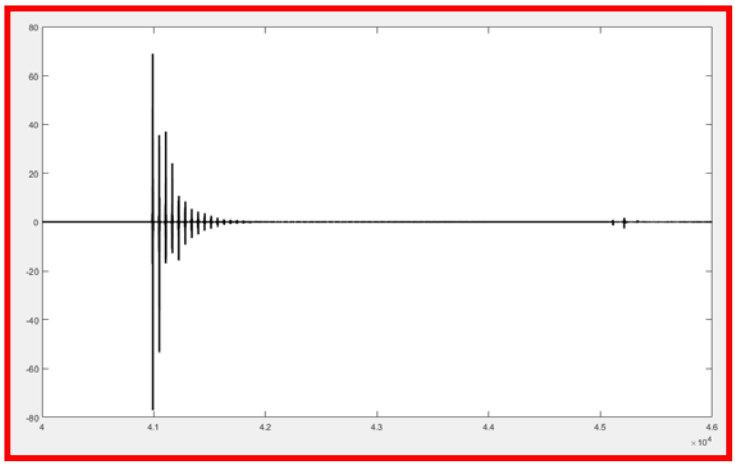

Figure 3.11 D1 variations (voltage signal) during the power swing

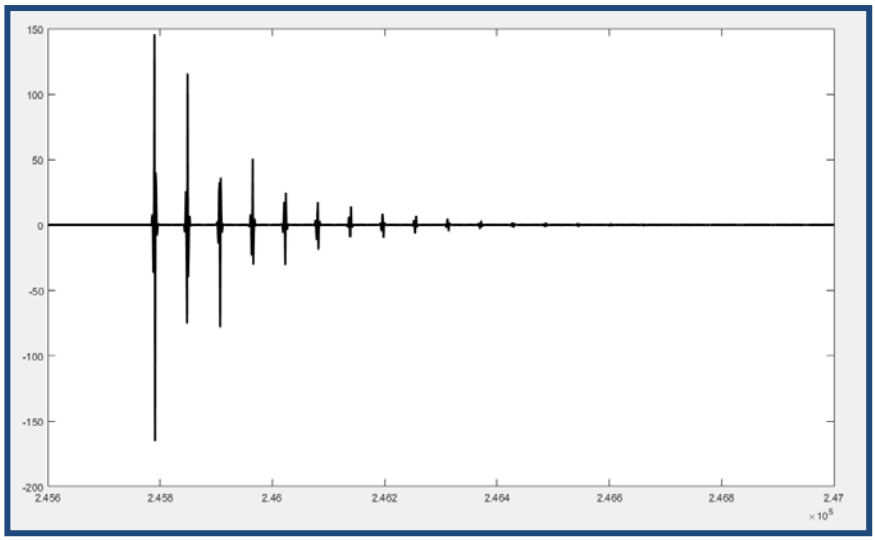

Figure 3.12 D1 variations (voltage signal) during the line-line fault

The current signal and its detail coefficients are shown Figure 3.13. The D1 coefficient of current in swing cycle is bigger than L-L fault condition. By choosing a threshold for this criterion the relay can detect the swing and be block by OSB function.

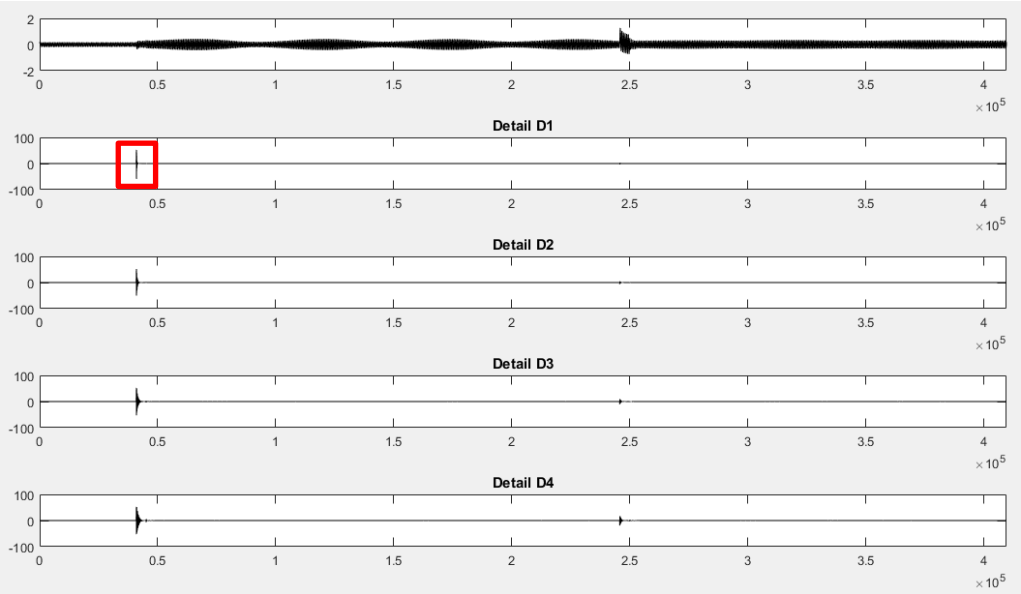

Figure 3.13 Relay terminal current signal and its 4-level detail coefficients

The D1 abrupt changes in the red rectangle during swing cycle is magnified in Figure 3.14.

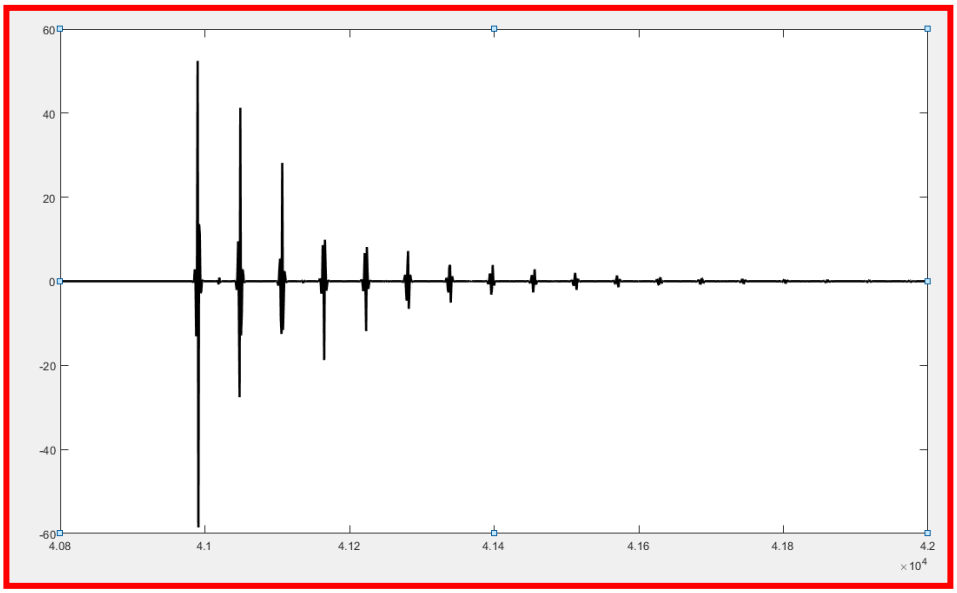

Figure 3.14 D1 variations (current signal) of relay current during the power swing

3.2 Power Swing Detection Techniques for Loss of Excitation Relays

As mentioned in the chapter 1, Bredy proposed the negative-offset mho characteristics for loss of excitation protection of the synchronous generators. Besides the impedance based LOE protection scheme which is the most popular one in industrial applications, there are also some other type LOE technique, such as impedance scheme enhanced with directional element, admittance scheme

(G-B plane), and active power- reactive power (P-Q) scheme or V-I one [17], and [28]. Based on the operation condition and fault location and types, the traditional LOE relay may detect the power swing as the fault and mis-operates. In [29] fuzzy logic-based technique which utilizes the impedance trajectory and generator terminal voltage to improve the conventional method is proposed which requires comprehensive simulation studies. In [30] the derivative of voltage and reactive power is utilized to detect generator LOE. This technique has a time delay and may misoperate with highly loaded generator during stable swing condition.

In addition a setting-free approach is presented in [31] that the rate of change of resistance variations at the generator terminal is introduced as the LOE detector. In the following section this technique is explained and its performance is studied on the test system.

3.2.1 Monitoring the Rate of Change of Apparent Resistance (*dR/dt*) to Detect LOE

In [31], a new algorithm for detecting LOE from power swing is proposed. The rate of change of generator terminal resistance is measured and if its value is negative and remains negative more than a specific time period, the generator suffers from loss of excitation. The apparent impedance at the generator terminal in the single machine infinite bus system (Figure 3.15) can be defined as Eq. (3.1) and (3.2) [31]:

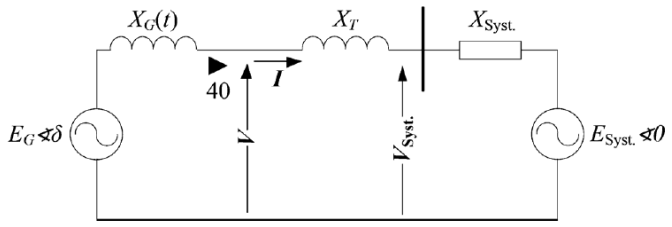

Figure 3.15 Thevenin equivalent circuit of power system

$$Z = \frac{k\sin\delta(t)}{1+k^2-2k\cos\delta} X_{Tot}(t) + j\left(\frac{1-k\cos\delta}{1+k^2-2k\cos\delta} X_{Tot}(t) - X_G(t)\right) \tag{3.1}$$

$$R(t) = \frac{k\sin\delta(t)}{1+k^2-2k\cos\delta} X_{Tot}(t)$$
$$X(t) = \frac{1-k\cos\delta}{1+k^2-2k\cos\delta} X_{Tot}(t) - X_G(t) \tag{3.2}$$

Where, $X_{Tot} = X_G(t) + X_T + X_{Sys}$, and $k(t) = E_{Sys} / E_G$. It is assumed the angle δ is constant when LOE occurs then *k* starts increasing. *dR/dt* is:

$$\frac{dR}{dt} = \frac{(1-k(t)^2)\sin\delta}{(1+k(t)^2-2k(t)\cos\delta)^2}\frac{dk}{dt}X_{Tot}(t) + \left(\frac{k(t)\sin\delta}{1+k(t)^2-2k(t)\cos\delta}\frac{dX_{Tot}(t)}{dt}\right) \quad (3.3)$$

Since *k* increases, *dk/dt* is positive. Therefore, as long as *k* is less than 1 (*k<1*), the first term will be positive. Since X_G changes during this period it is not possible to judge the sign of the second term. However, after a few seconds when X_G settles to its final value, the second term in (3.3) will become zero (*dX/dt=0*). At this time, *k* has increased far more than 1 (*k>1*) while *dk/dt* still remains positive. Therefore, after a period of time, the first term will become and remain negative and so will *dR/dt*. As a result, the relay will observe the rate of change of *R* and if *dR/dt* becomes and remains negative for a while, LOE can be detected.

During a power swing, similar condition can occur which means that *dR/dt* becomes and remains negative for a while. To distinguish the LOE from the power swing, it is then necessary to determine for how long *dR/dt* will remain negative during power swing at the worst case. The slip frequency is between 0.3 -7 Hz during swing period.

Thus, the longest period of *dδ/dt* that can be expected during a slowest power swing is 1/0.3=3.33 seconds, in half of this period, *dδ/dt* remains positive and *dR/dt* will not remain negative for more than 1.67 sec. To distinguish an LOE from the power swings, LOE relay should wait for 1.67 seconds and if still remains negative, an LOE can be detected.

- Simulation results

A SMIB system like Figure 3.3 is modeled in Matlab Simulink. The voltage and current phasors at the generator terminal are calculated, and then apparent *R*, *X*, *dR/dt* and *dx/dt* at relay are calculated in phasor domain.

1. LOE condition

LOE fault is modeled by changing the dc voltage input signal Vf of the generator. At t=4 s, Vf is changed to zero, so the generator lost its field. The dR/dt is depicted during fault period in Figure 3.16. As it is clear dR/dt in this condition became negative (before the fault dR/dt is zero) and remains in the negative section. After 1.7 s, LOE is detected and a trip signal will be sent to the generator circuit breaker at 5.7 s as shown in Figure 3.17.

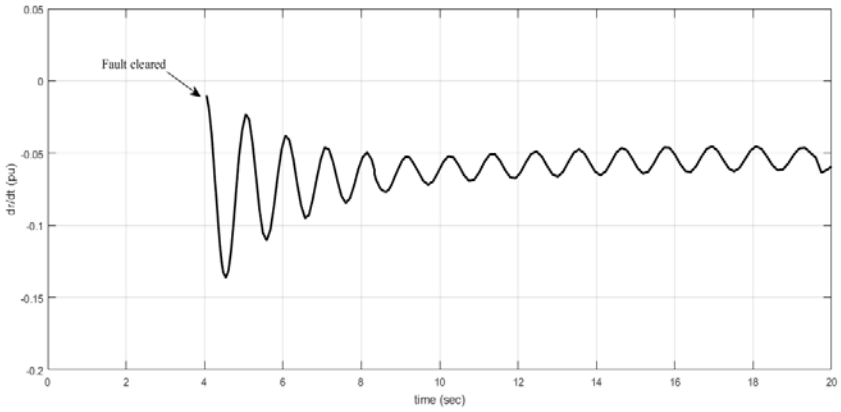

Figure 3.16 Variations of dR/dt measured by generator relay after LOE

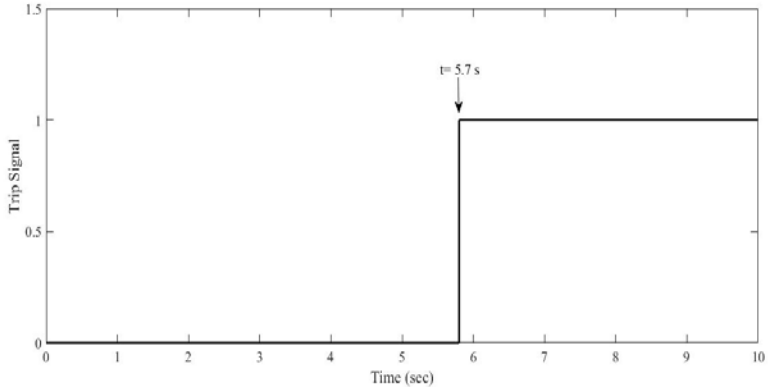

Figure 3.17 LOE Trip signal issued at 5.7 s

On the other hand, after LOE the impedance locus enters the conventional LOE characteristic of the relay. Impedance enters the zone#2 at 6.44 s and after 0.7 s (zone#2 delay+ breaker delay), the trip signal will issue at 7.14 s. the impedance locus and the trip signal instant are depicted in Figure 3.18 and Figure 3.19, respectively.

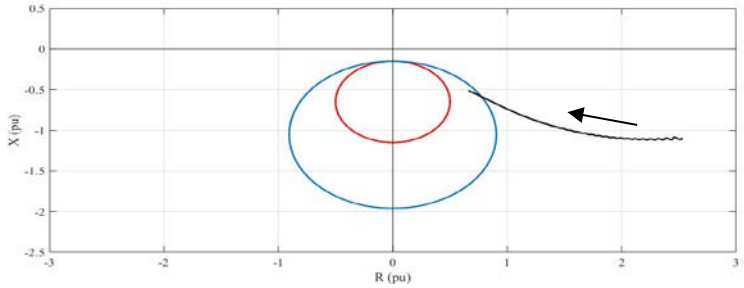

Figure 3.18 Impedance locus after LOE- conventional LOE characteristic

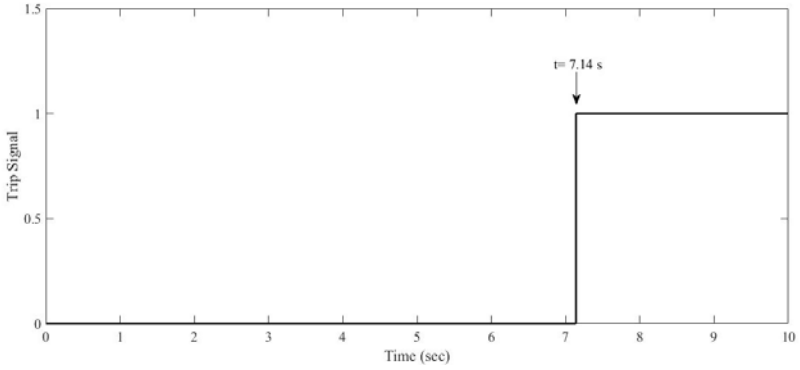

Figure 3.19 LOE Trip signal issued at 7.14 s- conventional LOE characteristic

2. Power swing condition

A fault is applied at the middle of the lower tie-line, and cleared after 5 cycle (fault occurs at 6 sec and cleared after 0.1 sec), the system experiences stable power swing. dR/dt variation is shown in Figure 3.20. *dR/dt* changes in the positive and negative planes. The slip frequency of this simulated swing condition is 0.7 Hz (1/1.3 s) which is one of the slowest power swings. It remains negative for half a cycle (0.65 sec) and then become positive. By this variation, the relay detects this condition as the stable swing and does not trip the generator.

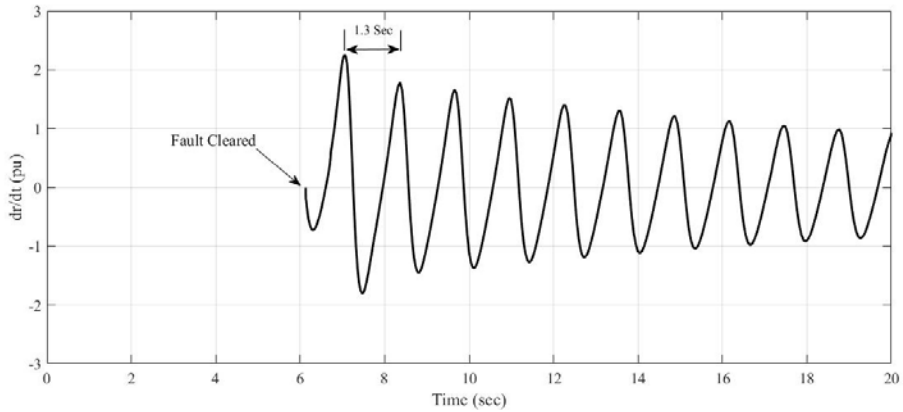

Figure 3.20 Variations of *dR/dt* measured by generator relay during power swing

3. LOE occurrence during swing condition

If during a stable swing a fault happened in the generator excitation system, the LOE relay should detect it and operate. A short circuit fault applied in the field circuit and V_f becomes zero at 10 sec, the *dR/dt* changes are shown in Figure 3.21. By LOE, *dR/dt* remains negative, after 1.7 s, trip signal will be sent at t= 11.7 s as shown in Figure 3.22.

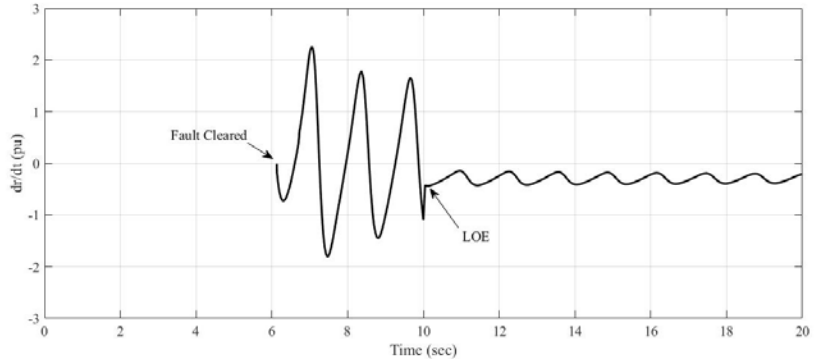

Figure 3.21 Variations of dR/dt measured- LOE during swing

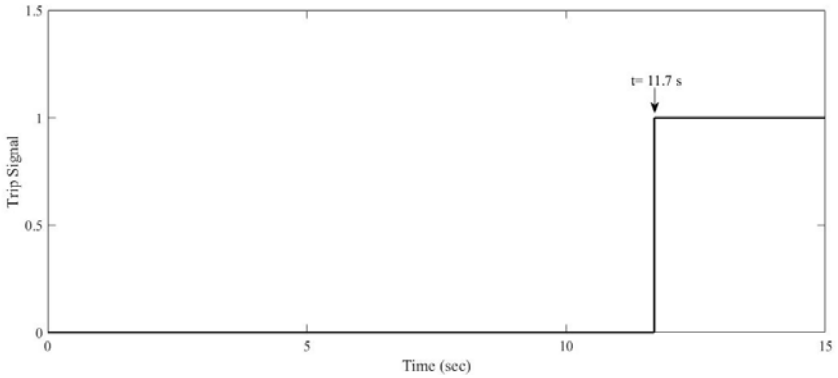

Figure 3.22 LOE Trip signal issued at 11.7 s

With respect to the conventional LOE characteristic, the impedance locus enters zone#2 at 12.83 s and after 0.7 s (zone#2 delay+ breaker delay), the trip signal will issue at 13.53 s. The impedance locus and the trip signal instant are depicted in Figure 3.23 and Figure 3.24, respectively.

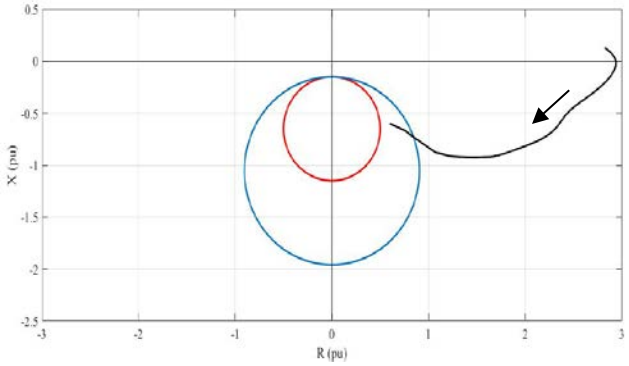

Figure 3.23 Impedance locus after LOE- conventional LOE characteristic

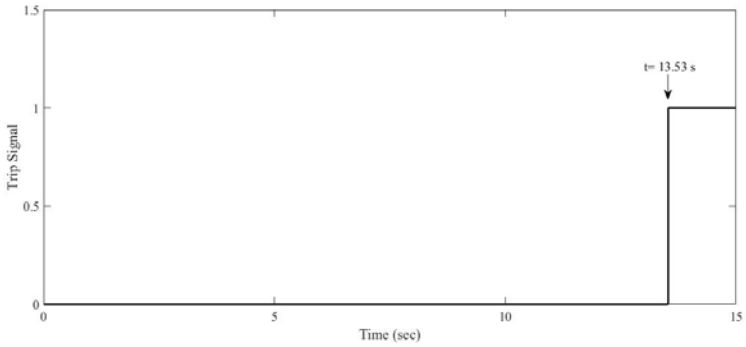

Figure 3.24 LOE Trip signal issued at 13.53 s- conventional LOE characteristic

The proposed method acts faster than the conventional 2 zone method and thus can isolate the generators suffering from LOE with less time delay. Since the measured resistance has an oscillatory nature due to the speed variation associated with slip frequency, this technique may not detect swing condition with the slow slip frequency [32].

3.3 Secure loss of excitation detection technique for synchronous generator

3.3.1 Principles of the proposed method

Synchronous generators as one of the significant equipment in the power system should be protected with highest rate of dependability, security and selectivity [33]. Thus, various types of protective relays such as differential relay (87G), ground fault protection (59GN and 27H), unbalanced current protection, loss of excitation protection (40),field ground protection (64F), out-of-step protection (78) and etc. are utilized to detect faulty conditions in the power supply rapidly, and prevent unwanted tripping of the generator [34].

The field circuit of synchronous generators keeps the generator synchronism with the power system by providing the required magnetizing energy. The excitation system establishes the rotor flux which generates the internal voltage of generators. Besides, the output reactive power of generator is dependent and changes by the internal voltage. The source tht excites the field winding may be interrupt due to incidents such as open or short circuit in the excitation system, equipment failure, inadvertent tripping of the field breaker, loss of field in the main exciter, a regulator control system failure, and slip ring flashover [31]. Following the occurrence of loss of excitation (LOE) the rotor current decays based on the field circuit time constant, as a result, the internal voltage of generator decreases with the same rate. Since the generator Var output is proportional to the internal voltage, it also decreases. The generator starts to absorb reactive power from the power system to replace the excitation previously provided by the field circuit. The reduction of the internal voltage causes voltage drops also weakens the coupling between rotor and stator. At some point during this period, active power cannot be transferred to the power system and the generator loses synchronism with the power system (loses synchronism torque). It can lead to high stator winding currents, severe pulsating torque, inducing AC voltage in field circuit, and stator end-core overheating. Moreover, the large amount of the Var absorbed by the generator from the system may jeopardize the voltage stability of the power system which can contribute to a wide area

system voltage collapse. Thus, the protective relays should detect the LOE quickly and accurately.

The effects of loss of synchronism resulted by a LOE event for the equivalent system shown in Figure 3.25, can be visualized based on the power angle equation. The active power injected to the system is defined based on the following equation:

$$P_e = \frac{E_I E_S}{X_d + X_{Sys}} \sin\delta + \frac{E_S^2 (X_d - X_q)}{2(X_d + X_{Sys})(X_q + X_{Sys})} \sin 2\delta \tag{3.4}$$

Where P_e, E_I, E_S, X_d, X_q, X_{Sys} and δ denote the electrical power, internal voltage, equivalent system voltage, d and q axis synchronous impedance, system impedance ($X_{Sys} = X_S + X_L$), and angle between E_I, and E_S, respectively. Ignoring the effect of the saliency is ignored by assuming $X_G = X_d = X_q$, then the power angle equation is expressed as:

$$P_e = \frac{E_I E_S}{X_G + X_{Sys}} \sin\delta \tag{3.5}$$

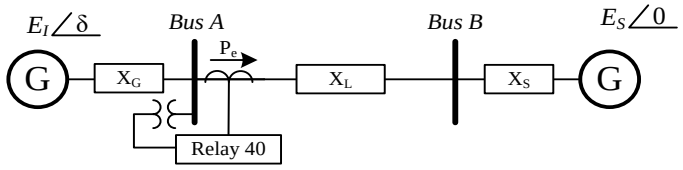

Figure 3.25 Thevenin equivalent circuit of power system

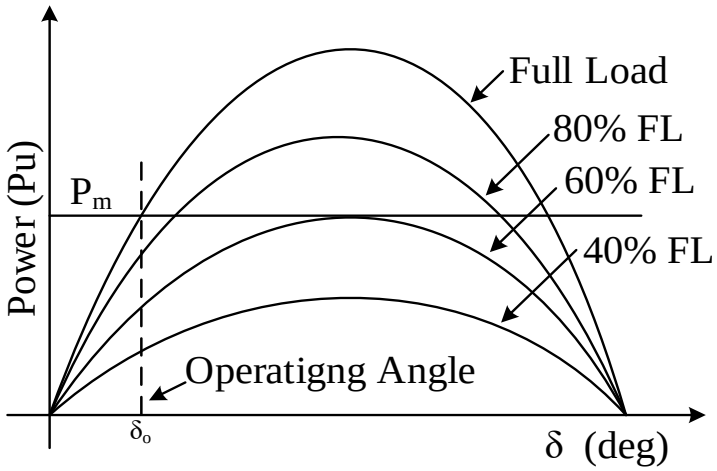

Figure 3.26 Power angle curve

As it is seen in the Figure 3.26 the intersection of the mechanical power of the turbine and the power angle curve define the operating angle of the generator with respect to the generator voltage. The delivered power to the system is proportional to the system and generator voltages and the sine of the angle difference between them. It is inversely proportional to the equivalent impedance of the network. During the LOE, the internal voltage decreases which leads to reduce the height of the power angle curve with time as shown by dotted curve. To maintain the equilibrium between the mechanical input (P_m) of the turbine and electrical output, the operating angle (δ) increases up to reaches the 90° which the electrical power is at maximum. Any decay in the field current after this point the generator loses its capability to transmit all the mechanical power to the power grid. The extra mechanical power increases the kinetic energy of the rotor and accelerating the shaft speed. As the angular speed rises over synchronous speed (60 Hz), the generator pull out of step and its synchronism is lost. The loss of synchronism is not a high-speed event, it is typically take a fully loaded generator several seconds to go out of step. So the out of step relay (78) can detect the loss of synchronism and trip the generator. During LOE period, the slip frequency for a machine at full load is typically at most in the range of 2-5% range. However, it is between 0.1-0.2% for light loaded generators [34].

During the LOE condition, the generator variables (E_I, X_G, and δ) changes with time while the system variables (E_S, and X_{Sys}) are almost constant, so the output power of generator can be expressed as follows:

$$P_e(t) = \frac{E_s^2 k(t)}{X_T(t)} \sin\delta(t) \tag{3.6}$$

Where

$$k(t) = \frac{E_I(t)}{E_S} \tag{3.7}$$

$$X_T = X_G(t) + X_{Sys} \tag{3.8}$$

Based on the aforementioned reasons, the generator maintains its active power equal to the mechanical input power during LOE before pulling out-of-step, so the rate of change of power (dP_e/dt) can be assumed equal zero in this period.

$$\frac{dP_e}{dt} = \frac{E_s^2}{X_T(t)} \frac{dk(t)}{dt} \sin\delta(t) + \frac{E_s^2 k(t)}{X_T(t)} \frac{d\delta}{dt} \cos\delta(t) - \frac{E_s^2 k(t)}{X_T(t)^2} \frac{dX_T(t)}{dt} \sin\delta(t) \tag{3.9}$$

From LOE occurrence, X_G moves toward the fourth quadrant with final value between the average of the d and q-axis subtransient reactances ($(X_d^{"} + X_q^{"})/2$) and the average of the d and q-axis synchronous reactances ($(X_d + X_q)/2$) [15]. Based on the initial loading of the generator, after some seconds, when the generator turns to a sink of reactive power, the X_G settles to the final value in the negative plane, then the derivative of machine reactance becomes zero ($dX_G/dt=0$), so the third term in the (3.9) will become zero. Since dP_e/dt equals to zero, so the rate of change of angle can be expressed as:

$$\frac{E_s^2}{X_T(t)}\frac{dk(t)}{dt}\sin\delta(t) + \frac{E_s^2 k(t)}{X_T(t)}\frac{d\delta}{dt}\cos\delta(t) = 0 \tag{3.10}$$

$$\frac{d\delta}{dt} = -\frac{dk(t)}{dt}\frac{1}{k(t)}\tan\delta(t) \tag{3.11}$$

In this interval, k decreases which is always positive, and dk/dt is negative. Besides, the operating angle (δ) is less than 90° , so the tan (δ) is positive, as a result, after LOE contingency, the generator operating angle always increases and its derivative (dδ/dt) becomes and remains positive and small before loss of synchronism.

During power swing, similar condition may happen which means the operating angle increases and dδ/dt becomes and remains positive for a few instants. According to the literature [22], and [35] the rate of change of angle dδ/dt oscillates with frequency between 1-7 Hz, also in [31] the slowest power swing is considered 0.3 Hz to guarantee the security issues. Thus during the swing condition dδ/dt sign will not remain positive and become negative after half a cycle as illustrated in Figure 3.27.

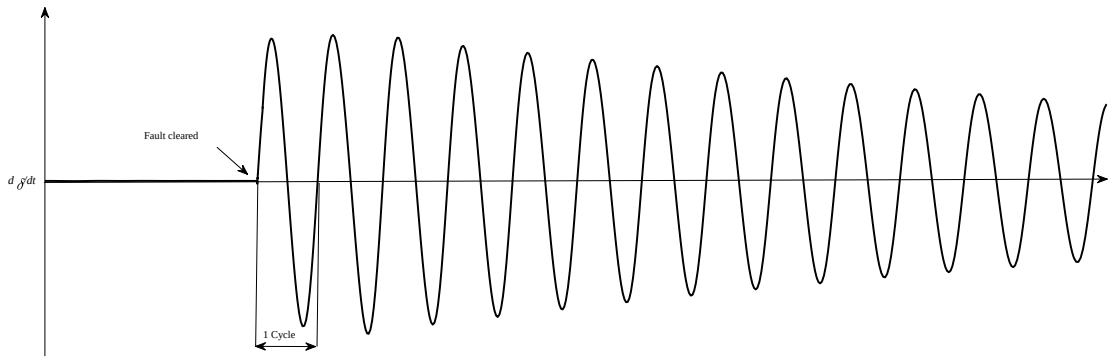

Figure 3.27 Oscillation of *dδ/dt* during the power swing condition

Moreover, as explained beforehand, during power swing condition, the slip frequency (*dδ/dt*) is in the range 0.3-7 Hz, which is different from the genuine LOE event. Therefore, the frequency of the measured signal can be utilized to discriminate between these two phenomena.

3.3.2 Defining the LOE detection delay (TD)

After the relay detects a disturbance at its terminal, if the dδ/dt remains positive for more than a half a cycle, the proposed method detects the LOE contingency. So a time delay (TD) is defined to guaranty the security of the detection algorithm. TD is defined based on the half cycle of the measured swing frequency (TSW) as follows (5% margin is also considered for security):

$$TD \geq 1.05 \times \frac{T_{SW}}{2} \tag{3.12}$$

or the sample rate (*S*) can be calculated as:

$$S \geq 1.05 \times \frac{f_S}{2 f_{SW}} \tag{3.13}$$

where f_{SW} and f_S denote the swing frequency and sampling frequency (which is typically 1kHz) [32]. The maximum time delay after disturbance detection is *TD*. For instance for the slowest power swing 0.3 Hz *TD* equals 1.75 s.

3.3.3 Logic of the proposed algorithm

Figure 3.28 shows the flowchart of the proposed method. Initially, the LOE relay (40) calculates the *P* and *dδ/dt* subsequently. The TD criterion is defined based on the half a cycle of the calculated slip frequency. Once the *dδ/dt* is non-zero a contingency is detected by the protection system, then if the slip frequency is out of swing frequency range and becomes and remains positive for more than predefined time delay (TD), the conventional relay (40) will operate and trip the generator. However, if the slip frequency is in the swing frequency range, it is distinguished as the swing event and the LOE relay will be blocked before the apparent impedance enters the mho characteristics of the LOE Relay.

If the relay estimates the slip frequency inaccurately and does not detects the swing frequency out of its typical range correctly, it will check the sign of rate of change of angle for TD period and correct its decision and block the mho zones. The proposed algorithm does not need any system parameters. The slip frequency is estimated based on the measured signal. While the other setting-free methods utilized the slowest swing (0.3 Hz) for the predefined time delay [31], [32].

3.3.4 Simulation results

Single machine infinite bus system is modeled in Matlab Simulink (Figure 3.29). The studied generator has the rated power of 600 MVA, and rated voltage 22 kV. The excitation model and system data are described in Appendix. To evaluate the performance of the proposed method, the generator in different initial loading conditions in lagging and leading power factor are investigated.

1. Generator heavy loading condition with lagging positive PF (L_1= 0.9+j0.3 p.u.)
    a. LOE condition

The excitation system of the generator is short circuit at t=2 s and the dc field voltage changes to zero. Since the generator lost its exciter, the output reactive power decays while the active power is still constant at its initial value. The output active and reactive powers of generator are depicted in Figure 3.30.

The polarity of the rate of change of power angle (δ) is always positive during loss of excitation. The trajectory of the power angle variations is always in the first quadrant of the $d\delta$-δ plane as illustrated in Figure 3.31.

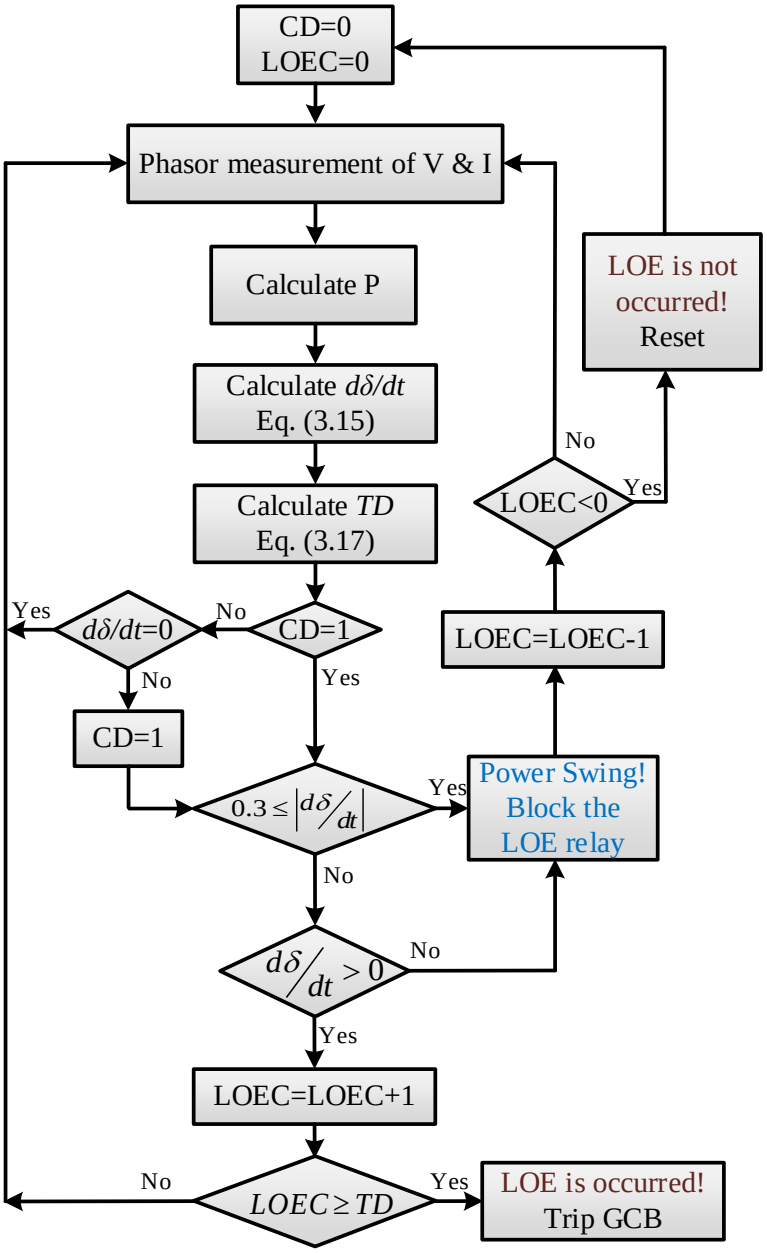

Figure 3.28 Flowchart of the proposed adaptive LOE detection technique

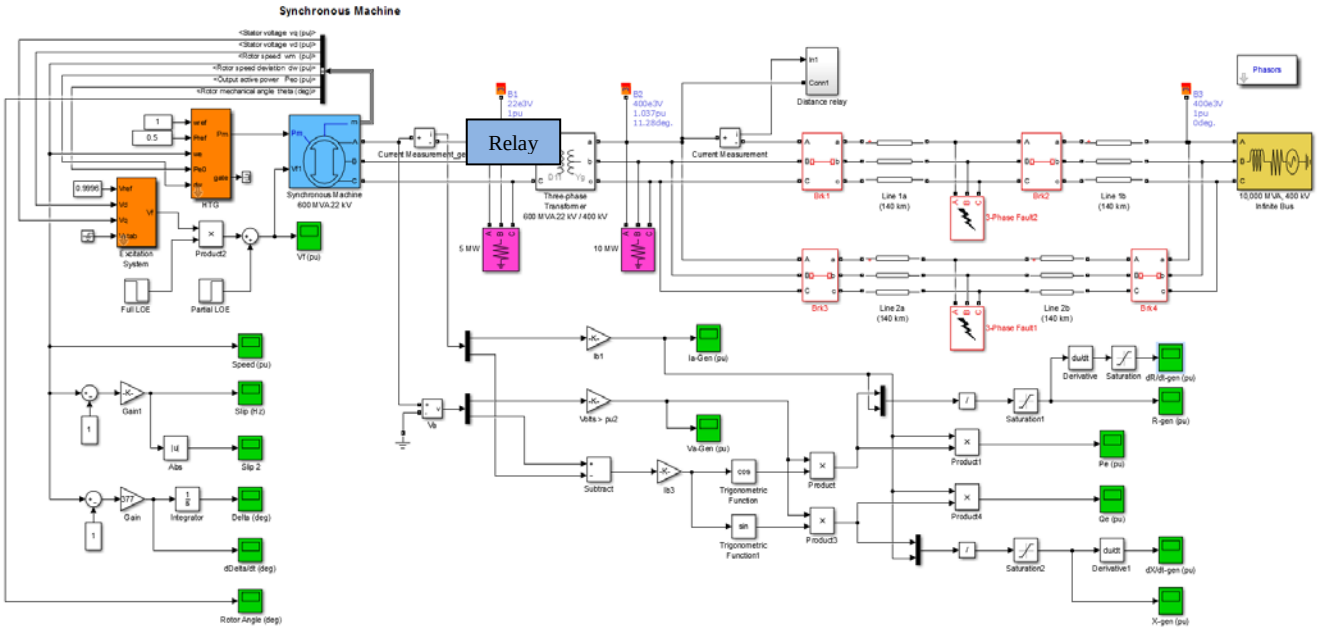

Figure 3.29 Single machine infinite bus system

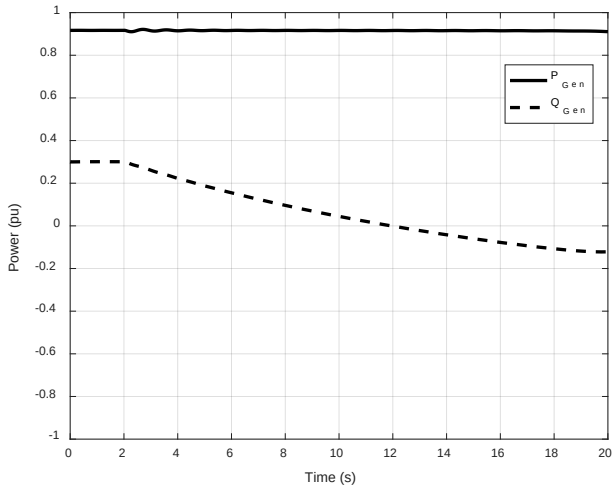

Figure 3.30 Active and reactive powers of synchronous generator following LOE- L_1 loading condition

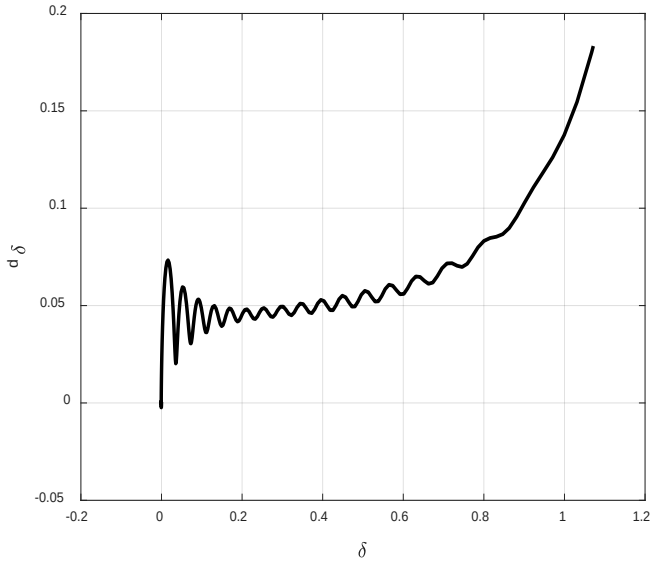

Figure 3.31 Variation of generator angle during LOE occurrence- L_1 loading condition

Also, the slip frequency for this loading condition is less than the typical swing frequency as shown in Figure 3.32, it is close to zero value.

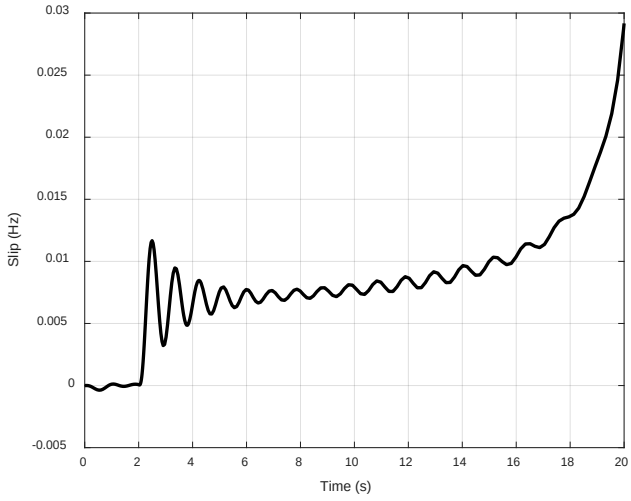

Figure 3.32 Slip frequency variation during LOE occurrence- L_1 loading condition

Based on the calculated variables, the proposed algorithm detects this contingency as LOE after half a cycle and will not block the relay. Then the apparent impedance at relay location moves toward the third quadrant of the R-X plane after loss of excitation. It enters zone2 and zone 1 of the relay at 8.56 s and 9.03 s, respectively. The typical pre-defined time delay for zone 1 LOE is 0.1 s (the breaker operating time is 0.05 s), so the generator disconnected from the grid at 9.18 s

by the zone 1 of LOE relay. The impedance locus and the trip signal instant are depicted in Figure 3.33 and Figure 3.34, respectively.

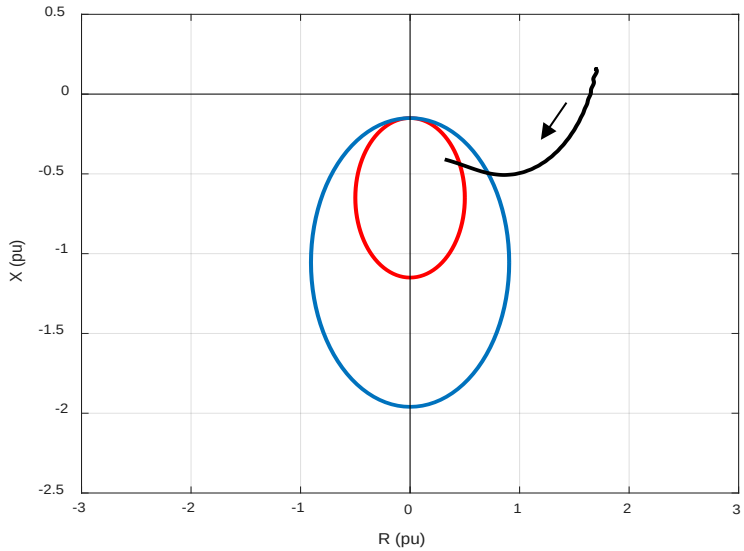

Figure 3.33 Apparent impedance locus during LOE occurrence- L_1 loading condition

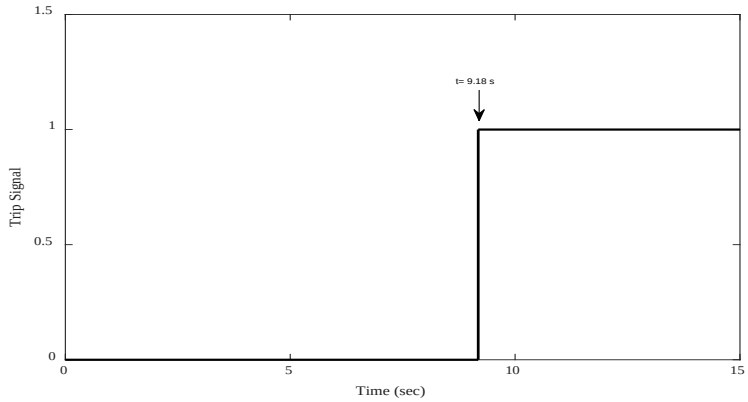

Figure 3.34 LOE Trip signal issued at 9.18 s

b. Power swing condition

If a fault occurs at the middle of the lower tie-line on the system shown in Figure 3.29, at t= 4 s and cleared after 0.1 s by tripping the faulted line, the generator oscillates to get the new equilibrium point. The active and reactive output powers of the generator are shown in Figure 3.35. The reactive power oscillates around the new positive output power. The angle (δ) is non-monotonic during the power swing and the rate of change of angle $d\delta$ changes between positive and negative values. The trajectory of the power angle variations is illustrated in the $d\delta$-δ plane in Figure 3.36. The angle locus starts from origin and rotates in the negative and positive side of this

plane to reach to the new operating point for stable power swing. The polarity of the $d\delta$ changes after every half cycle.

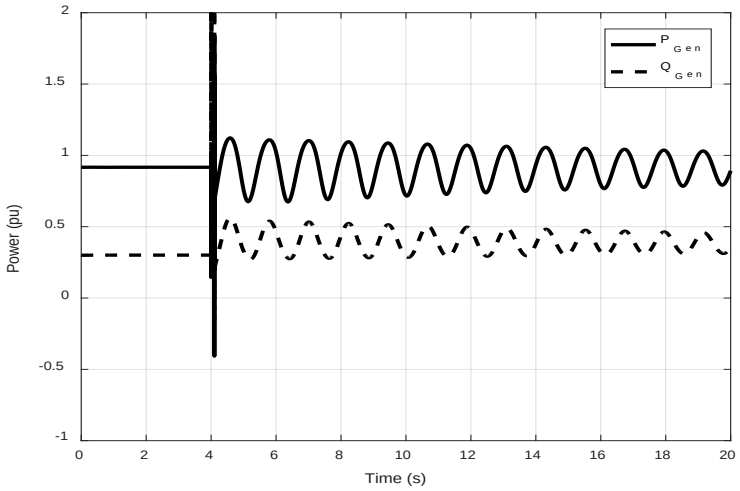

Figure 3.35 Active and reactive powers of synchronous generator during power swing- L_1 loading condition

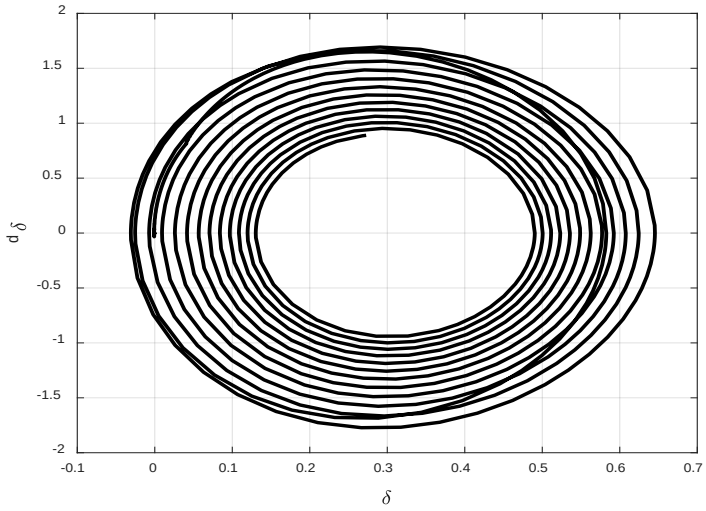

Figure 3.36 Variation of generator angle during power swing- L_1 loading condition

Besides, the slip frequency for this loading condition is more than 1 Hz and the proposed algorithm detects this condition as the power swing and blocks the relay correctly. The stable power swing is shown in Figure 3.32.

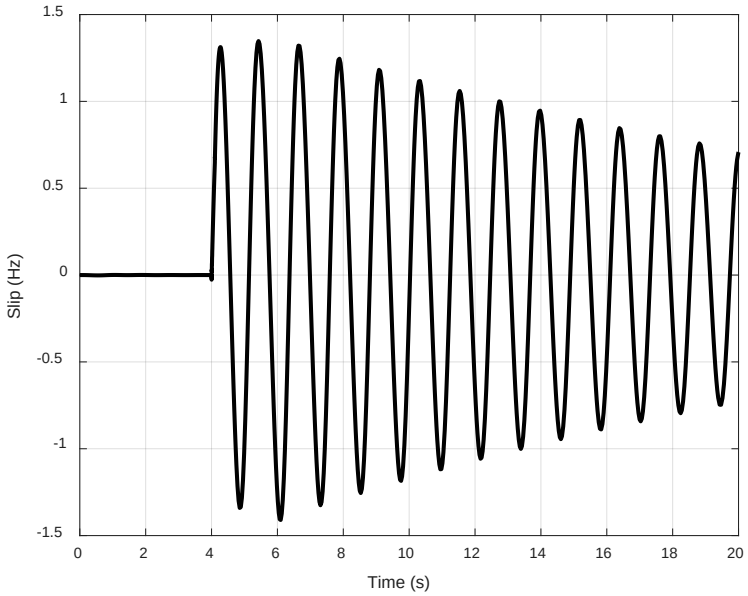

Figure 3.37 Slip frequency variation during stable power swing- L_1 loading condition

2. Generator height loading condition with leading positive PF (L_2= 0.4-j0.35 p.u.)
   a. LOE condition

Similar to tthe previous loading condition, the excitation system of the generator is short circuit at t=2 s. Since the generator lost its exciter, the output reactive power decays while the active power is still constant at its initial value. The output active and reactive powers of generator are depicted in Figure 3.38.

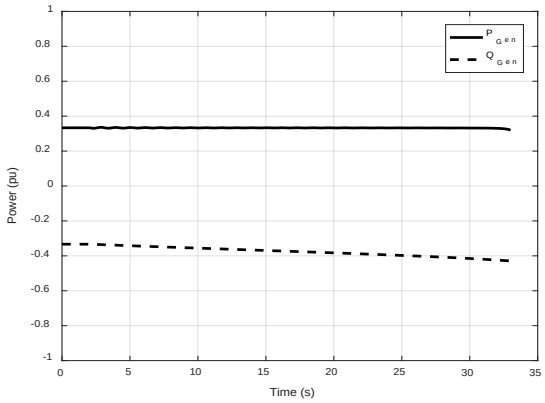

Figure 3.38 Active and reactive powers of synchronous generator following LOE- L_2 loading condition

The polarity of the rate of change of power angle (δ) is always positive during loss of excitation. The trajectory of the power angle variations is always in the first quadrant of the dδ-δ plane as illustrated in Figure 3.39.

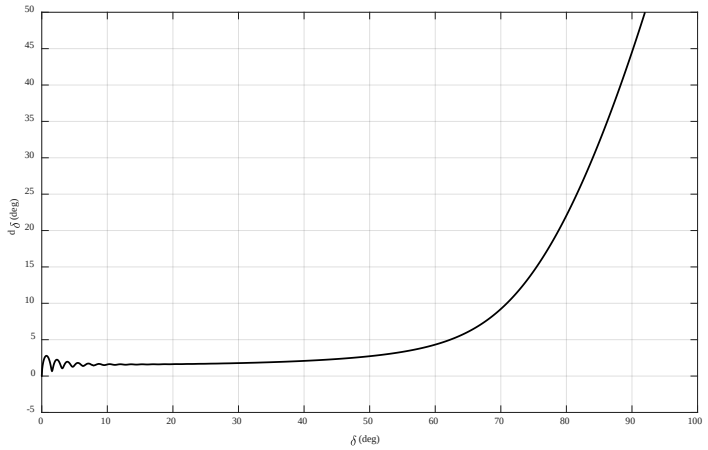

Figure 3.39 Variation of generator angle during LOE occurrence- L_2 loading condition

Also, the slip frequency for this loading condition is less than 0.05 Hz before losing the synchronism as shown in Figure 3.40.

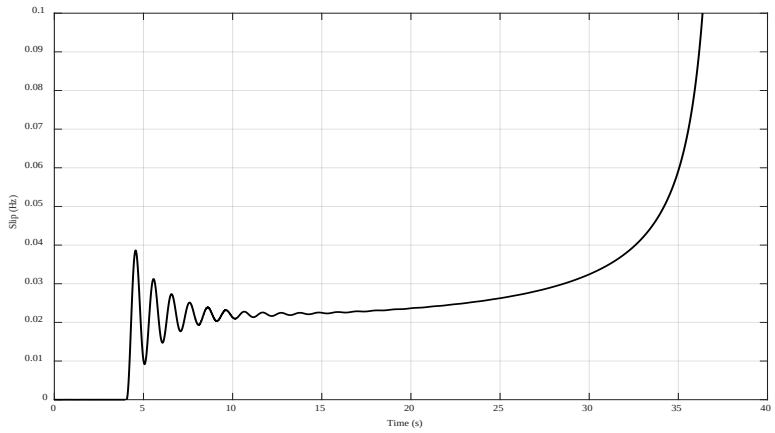

Figure 3.40 Slip frequency variation during LOE occurrence- L_2 loading condition

Based on the calculated variables, the proposed algorithm detects this contingency as LOE after half a cycle and will not block the relay. Since the generator is operated with the initial leading PF, the apparent impedance starts its trajectory from a point with negative reactance in the third quadrant of the R-X plane after loss of excitation. It enters zone2 and zone 1 of the relay at 14.24 s and 14.89 s, respectively. The typical pre-defined time delay for zone 2 LOE is 0.65 s (the breaker operating time is 0.05 s), so the generator tripped from the grid at 14.94 s by operating the zone 2 of the LOE relay. The impedance locus and the trip signal instant are depicted in Figure 3.41 and Figure 3.42, respectively.

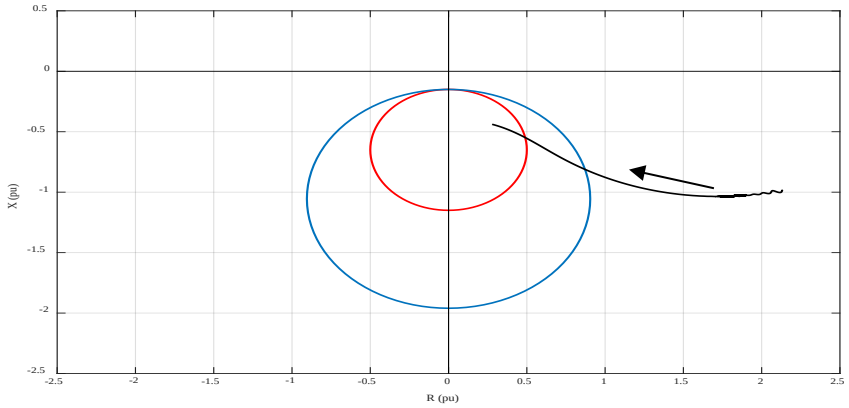

Figure 3.41 Apparent impedance locus during LOE occurrence- L_2 loading condition

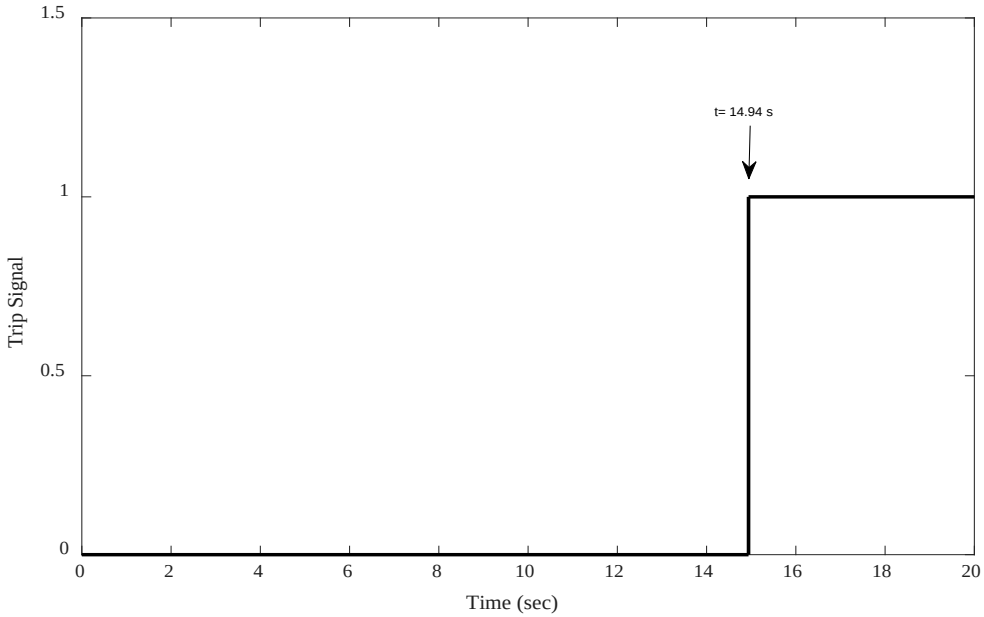

Figure 3.42 LOE Trip signal issued at 14.94 s

b. Power swing condition

A 3-phase fault applied on the lower tieline in single machine infinite bus system and cleared after 0.1 s by opening the line. The system experiences power swing. The active and reactive output powers of the generator are shown in Figure 3.43. The reactive power oscillates around the new negaticve output Var. The angle (δ) is non-monotonic during the power swing and the rate of change of angle $d\delta$ changes between positive and negative values. The trajectory of the power angle variations is illustrated in the $d\delta$-δ plane in Figure 3.44. The angle locus starts from origin

and rotates in the negative and positive side of this plane to reach to the new operating point for stable power swing. The polarity of the $d\delta$ changes in every half cycle.

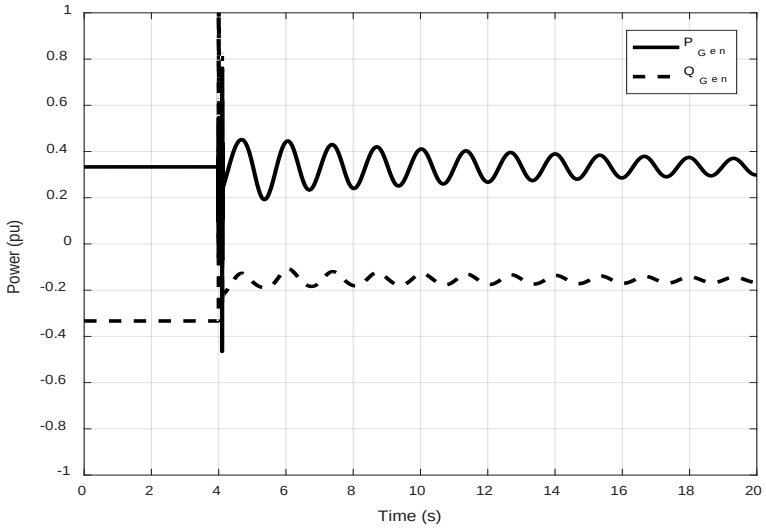

Figure 3.43 Active and reactive powers of synchronous generator during power swing- L_2 loading condition

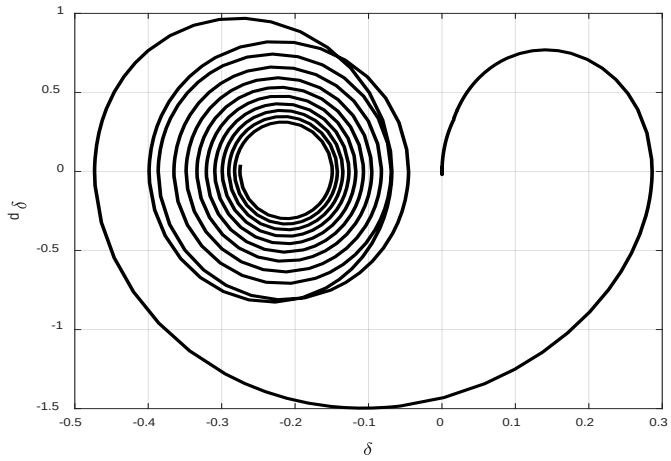

Figure 3.44 Variation of generator angle during power swing- L_2 loading condition

Besides, the slip frequency for this loading condition is more than 0.7 Hz and the proposed algorithm detects this condition as the power swing and blocks the relay correctly. The stable power swing is shown in Figure 3.45.

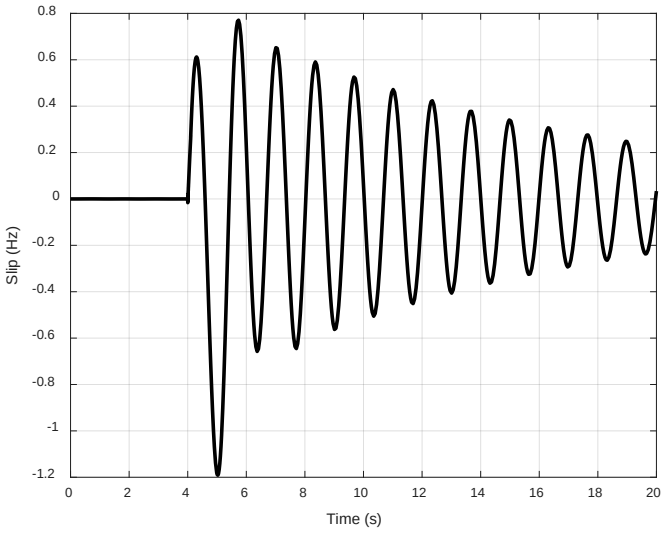

Figure 3.45 Slip frequency variation during stable power swing- L_2 loading condition

The investigated case studies with different generator initial loading conditions confirmed the accuracy of the proposed LOE strategy.

4. Conclusions

In this project, the dynamic simulation and protection model were linked in CAPE-PSS/E co-simulation platform in which all the protection devices (relays, breakers, VTs, and CTs) were modelled precisely. Mis-operation conditions of impedance elements of distance relay and loss of excitation (LOE) relay were investigated in the co-simulation platform. The simulation results demonstrated that under certain conditions these relays with the typical time delay and blocking settings may mis-operate.

The response of the distance relays in the WECC system model after the critical outages was examined. It can be concluded that failure in detecting mis-operating relays may result in a system-wide collapse.

Moreover, to prevent the LOE relay mis-operation during power swing a novel method was proposed. The rate of change of rotor angle and the machine slip frequency magnitude were utilized to distinguish the LOE from power swing. Conventional LOE relays can be enhanced by adding a logic block which is designed based on the proposed method to differentiate power swing from LOE condition. As a result of using the proposed method, LOE relays become more secure as mis-operation of the relays are prevented during power swing conditions.

The performance of the proposed method were evaluated using numerous test cases with different generator loading levels and the power factors active power some of which are reported in the case study results section.

The test system was simulated in CAPE-PSS/E co-simulation platform and the obtained results demonstrated that the proposed method can detect power swing conditions in half a cycle and block the relay from mis-operations.

Appendix:

The parameters of the test system used for co-simulation (Figure 2.4) are as follows:

Generator 1:

600MVA, 22 kV, 60 Hz, Inertia constant 4.4 MW/MVA

Xd= 1.8 pu, X'd=0.3 pu, X"d=0.23 p.u., T'd0= 8 s, T"d0=0.03 s, Ra= 0.003 p.u.

Transformer:

600 MVA, 22/400 kV Δ/Y, X=0.163 pu.

The transmission lines parameters are reported in Table. A. 1.

Table A.1 Transmission lines resistance and reactance

From bus	To bus	R (pu)	X (pu)
2	3	0.008	0.165
3	4	0.008	0.165
2	4	0.0165	0.325

The exciter is modelled by IEEE ESST1A type in PSS/E.

Table A.2 Parameter of exciter model

Parameter	Value	Parameter	Value
T_R (sec)	0.1	$V_{A\,MAX}$	4.6
$V_{I\,MAX}$	5	$V_{A\,MIN}$	-4.6
$V_{I\,MIN}$	-5	$V_{R\,MAX}$	3.4
T_C (sec)	0.01	$V_{R\,MIN}$	-3.4
T_B (sec)	240	K_C	0.01
T_{C1} (sec)	0.01	K_F	0.1
T_{B1} (sec)	0.1	T_F (sec)	0.1
K_A	1	KLR	1
T_A (sec)	0.01	ILR	2

CTs and VT with the CTR and VTR 120 and 1000 are located at the relays' locations, respectively. According to the CT and CT ratios, and impedance of the lines, the zone 1 and zone 2 of the line distance relays are defined as follows:

$$X_{Secondary} = \frac{kV^2 \times X_{primary}}{MVA} \times \frac{CTR}{VTR} \tag{4.1}$$

The typical time delays are used for the distance relays time settings. The LOE relay time delay is set 0.1 s for zone 1 and 0.75s for zone 2. Breaker operating time is 50 ms (3 cycles).

References:

[1] U.S.-Canada Power System Outage Task Force, "Final report on the August 14, 2003 blackout in the United States and Canada: Causes and Recommendations", April 5, 2004. [Online]. Available: http://www.nerc.com.

[2] J. J. Bian A. D. Slone, P. J. Tatro "Misoperations Report:Protection System Misoperations Analysis" *NERC Planning Committee*, April, 2013.

[3] "Standard PRC-004-3 — Protection System Misoperation Identification and Correction".

[4] D. Tziouvaras, "Relay Performance during Major System Disturbances".

[5] M. A., Khorsand, and V. Vittal, "Modeling Protection Systems in Time-Domain Simulations: A New Method to Detect Mis-operating Relays for Unstable Power Swings," submitted to *IEEE Trans. power sys.*, 2016.

[6] "Protection system response to power swings" *Syst. Protec. and Cont. Subcom., NERC*, Aug. 2013.

[7] M. Kezunovic, C. Pang, J. Ren, and Y. Guan, "New Solutions for Improved Transmission Line Protective Relay Performance Analysis,".

[8] S. A. Soman, T. B. Nguyen, M. A. Pai and R. Vaidyanathan, "Analysis of angle stability problems: a transmission protection systems perspective," *IEEE Trans. on Power Del.*, vol. 19, no. 3, pp. 1024-1033, July 2004.

[9] N. Zhang, H. Song and M. Kezunovic, "Transient based relay testing: a new scope and methodology," *IEEE Mediterranean Electrotechnical Conf. (MELECON)*, Malaga, pp. 1110-1113, 2006.

[10] S. A. Soman, T. B. Nguyen, M. A. Pai and R. Vaidyanathan, "Analysis of angle stability problems: a transmission protection systems perspective," *IEEE Trans. on Power Del.*, vol. 19, no. 3, pp. 1024-1033, July 2004.

[11] Q. Verzosa, "Realistic Testing of Power Swing Blocking and Out-of-Step Tripping Functions,".

[12] N. Fischer, G. Benmouyal, D. Hou, D. Tziouvaras, J. B. Finley, and B. Smyth, "Tutorial on Power Swing Blocking and Out-of-Step Tripping," 39th *Annual Western Protective Relay Conference*, Spokane, WA, Oct., 2012.

[13] U. N. Khan, and L. Yan, "Power Swing Phenomena and its Detection and Prevention," *7th EEEIC Int. Workshop on Environ. and Elec. Eng*., Cottbus, May 2008.

[14] "Generating Out-of-Step Blocking and Tripping Settings in the Computer-Aided Protection Engineering System (CAPE)," CAPE Users' Group, June, 2005.

[15] Yao Siwang, Wang Weijian, Luo Ling, Gui Lin , Qiu Arui, "Discussion on Setting Calculation of Loss-Of-Excitation Protection for Large Turbogenerator," *Int. Conf. on Elect. Mach. and Syst. (ICEMS)*, pp. 1413–1416, 2010.

[16] C. R. Mason, "New loss of excitation relay for synchronous generators," *AIEE Trans.*, vol. 68, no. 2, pp. 1240–1245, 1949.

[17] J. Berdy, "Loss of excitation protection for modern synchronous generators," *IEEE Trans. Power Appar. Syst.*, PAS-94, (5), pp. 1457–1463, 1975.

[18] C. J. Mozina, M. Reichard, "Coordination Of Generator Protection With Generator Excitation Control and Generator Capability," *IEEE Gen. Meeting* , 2007.

[19] E. Pajuelo, R. Gokaraju, M. S. Sachdev, "Identification of generator loss-of-excitation from power-swing conditions using a fast pattern classification method," *IET Generation, Transmission & Distribution*, Vol. 7, Iss. 1, pp. 24–36, 2013.
[20] IEEE Power System Relaying Committee working group, "Performance of Generator Protection During Major System Disturbances," *IEEE Trans. Power Delivery*, vol. 19, no. 4, pp. 1650–1662, October 2004.
[21] "PSS®E 33.5 Program operation manual" Siemens Oct. 2013.
[22] "CAPE Series CAPE-TS LinkTM Module User's Guide," Electrocon International, Inc, March 2015.
[23] S. M. Brahma, "Distance Relay With Out-of-Step Blocking Function Using Wavelet Transform," *IEEE Trans. Power Delivery*, vol. 22, no. 3, July 2007.
[24] T. E. Baker, " Electrical Calculations and Guidelines for Generating Station and Industrial Plants," Taylor and Francis Group, 2012.
[24] California ISO, "Transmission Plan" 2010-1011.
[26] G. Xu, V. Vittal, A. Meklin, and J. E. Thalman, "Controlled islanding demonstrations on the WECC system," *IEEE Trans. Power Syst.*, vol. 26, no. 1, pp. 334-343, Feb. 2011.
[27] Major WECC remedial action schemes (RAS), WECC, Available: https://www.wecc.biz/Reliability/TableMajorRAS4-28-08.pdf.
[28] "Power swing and out-of-step considerations on transmission lines," *report Power System Relaying Committee (PSRC)- IEEE PES*, July, 2005.
[29] Y. Siwang, W. Weijian, L. Ling, G. Lin and Q. Ami, "Discussion on setting calculation of loss-of-excitation protection for large turbo generator," *Int. Conf. Elect. Mach. and Sys.*, pp. 1413-1416, Incheon, 2010.
[30] A. P. de Morais, G. Cardoso and L. Mariotto, "An Innovative Loss-of-Excitation Protection Based on the Fuzzy Inference Mechanism," *IEEE Trans. on Power Del*, vol. 25, no. 4, pp. 2197-2204, Oct. 2010.
[31] M. Amini, M. Davarpanah and M. Sanaye-Pasand, "A Novel Approach to Detect the Synchronous Generator Loss of Excitation," *IEEE Trans Power Del.*, vol. 30, no. 3, pp. 1429-1438, June 2015.
[32] B. Mahamedi, J. G. Zhu and S. M. Hashemi, "A Setting-Free Approach to Detecting Loss of Excitation in Synchronous Generators," *IEEE Trans. on Power Del.*, vol. 31, no. 5, pp. 2270-2278, Oct. 2016.
[33] A. Hasani; F. Haghjoo, "A Secure and Setting-Free Technique to Detect Loss of Field in Synchronous Generators," *IEEE Trans. Energy Conv.*, vol.PP, no.99, pp.1-1, 2017.
[34] *IEEE Guide for AC Generator Protection*, *IEEE* Standard C37.102- 2006, Nov. 2006.
[35] D. Reimert, "Protective Relaying for Power Generation Systems," 3rd edition, Taylor & Francis, 2006.
[36] G. Benmouyal, D. Hou, and D. Tziouvaras, "Zero-setting power-swing blocking protection,"[Online].Available: http://www.selinc.com/ techpprs/6172_ZeroSetting_ 20050302.pdf